ELSEVIER

A reduced mathematical model of the acute inflammatory response II. Capturing scenarios of repeated endotoxin administration

Judy Day[a], Jonathan Rubin[a,*], Yoram Vodovotz[b,c,d], Carson C. Chow[e], Angela Reynolds[a], Gilles Clermont[f,c,d]

[a]*Department of Mathematics, 301 Thackeray, University of Pittsburgh, Pittsburgh, PA 15260, USA*
[b]*Department of Surgery, University of Pittsburgh Medical Center, W1542 Biomedical Sciences Tower, 200 Lothrop St., Pittsburgh, PA 15213, USA*
[c]*Center for Inflammatory and Regenerative Medicine (CIRM), 100 Technology Drive Suite 200, Pittsburgh, PA 15219-3110, USA*
[d]*CRISMA Laboratory, University of Pittsburgh, Pittsburgh, PA 15261, USA*
[e]*Laboratory of Biological Modeling, NIDDK, NIH, Bethesda, MD 20892, USA*
[f]*Department of Critical Care Medicine, 3550 Terrace St, University of Pittsburgh Medical Center, Pittsburgh, PA 15261, USA*

Abstract

Bacterial lipopolysaccharide (LPS; endotoxin) is a potent immunostimulant that can induce an *acute inflammatory response* comparable to a bacterial infection. Experimental observations demonstrate that this biological response can be either blunted (tolerance) or augmented (potentiation) with repeated administration of endotoxin. Both phenomena are of clinical relevance. We show that a four-dimensional differential equation model of this response reproduces many scenarios involving repeated endotoxin administration. In particular, the model can display both tolerance and potentiation from a single parameter set, under different administration scenarios. The key determinants of the outcome of our simulations are the relative time-scales of model components. These findings support the hypothesis that endotoxin tolerance and other related phenomena can be considered as dynamic manifestations of a unified acute inflammatory response, and offer specific predictions related to the dynamics of this response to endotoxin.

© 2006 Elsevier Ltd. All rights reserved.

1. Introduction

The initial response of the body to acute biological stress such as bacterial infection or tissue trauma is an *acute inflammatory response*. This response involves a cascade of events mediated by a large array of cells and molecules that locate invading pathogens or damaged tissue, alert and recruit other cells and effector molecules, eliminate the offending agents, and restore the body to equilibrium. Bacterial lipopolysaccharide (*LPS; endotoxin*) is a highly conserved, highly immunogenic, constituent molecule of the outer cell wall of Gram-negative bacteria. When bacteria are lysed by immune effector cells and molecules,

surges of endotoxin may be released into the host, intensifying the inflammatory response and causing further activation of immune effector cells (Alexander and Rietschel, 2001; Janeway and Medzhitov, 2002). In fact, the administration of antibiotics can lead to pulses of endotoxin release from Gram-negative bacteria as the antibiotics kill the invading bacteria, confirming the clinical importance of this subject matter (Eng et al., 1993). Since direct endotoxin administration in animals and humans can induce an acute inflammatory response that reproduces many of the features of an actual bacterial infection, such as fever, it stands as a valid experimental model for investigating the inflammatory response (Copeland et al., 2005; Morrison and Ryan, 1987; Parrillo, 1993).

High doses of endotoxin can be lethal, even though this bacterial byproduct does not proliferate as a Gram-negative

---

*Corresponding author. Fax: +1 (412) 624 8397.
E-mail address: rubin@math.pitt.edu (J. Rubin).

bacteria would (Senaldi et al., 1999). It has been observed, however, that in some instances repeated doses of endotoxin result in a considerably less vigorous immune response, a phenomenon referred to as endotoxin tolerance (Beeson, 1947). In fact, the induction of tolerance can greatly blunt the effect of a dose of endotoxin that would be lethal to a naïve animal. A variety of studies have followed up on Beeson's initial reports of endotoxin tolerance (for a historical perspective see Cross, 2002; Schade et al., 1999; West and Heagy, 2002). Experimentally, it is now possible to assess the activation status of inflammatory cells or the levels of signaling proteins, such as cytokines, in organs or the blood as direct measures of inflammation (Nathan, 2002; Nathan and Sporn, 1991). The cytokine *Tumor Necrosis Factor-α* (*TNF*) in blood serum, for instance, has become a prominent marker of inflammation (Janeway et al., 2001; Sanchez-Cantu et al., 1989). Thus, observing that the concentration of this cytokine is lower than levels normally observed after endotoxin administration suggests that inflammation is being suppressed.

Interestingly, the inverse phenomenon, called potentiation, has also been observed. In the extreme, an otherwise non-lethal dose of endotoxin rapidly following another non-lethal dose can result in death (Cavaillon, 1995). We hypothesized that a simple mathematical model of the acute inflammatory response could reconcile tolerance and potentiation, on the premise that the observed outcomes result from dynamic interactions between components of innate immunity. Accordingly, we adapted a recently developed computational model of the inflammatory response (Reynolds et al., 2006) and simulated various scenarios involving repeated endotoxin administration. We use actual experimental mouse scenarios to guide in silico experiments that recreate these scenarios qualitatively, including the phenomena of endotoxin tolerance and potentiation.

In our simulations, we find that both the timing and magnitude of endotoxin doses, relative to each other and to the dynamical interplay between pro- and anti-inflammatory mediators, is the key to discriminating between the seemingly disparate phenomena of endotoxin tolerance and potentiation. Our results, derived from a mathematical model not constructed specifically to address the issue of preconditioning, support the perspective that endotoxin tolerance and related phenomena could be better explained and understood as "inflammatory-stimuli-induced" effects rather than specific, distinct phenomena (Cavaillon, 1995). This perspective is also supported by studies showing that various inflammatory stimuli (e.g. trauma, hemorrhage, cytokines) can act either to tolerize or to prime the host for subsequent homologous or heterologous stimuli (Bumiller et al., 1999; Cavaillon et al., 1994; Kariko et al., 2004; Keel et al., 1996; Leon et al., 1992; Mendez et al., 1999; Vogel et al., 1988; Zervos et al., 1999). The intent of this paper is not to carry out a detailed mathematical analysis of our model. Rather, we hope to argue convincingly that endotoxin tolerance, potentiation, and other phenomena related to

repeated endotoxin administration are best viewed and understood via the acute inflammatory response (Copeland et al., 2005; Yadavalli et al., 2001) and to demonstrate this with a mathematical model of that response.

2. A mathematical model of the acute inflammatory response to endotoxin

To examine repeated endotoxin administration in the context of the acute inflammatory response, we use a mathematical model that incorporates the effects of key aspects of the immune system's response to an insult (Eqs. (1)–(4)). The detailed derivation of this model, based on previous experimental findings, and a term-by-term explanation of its components are outlined by Reynolds et al. (2006). The model we use replaces the pathogen equation of Reynolds et al. with an endotoxin equation. These changes introduce several different parameters that replace or add to those used in Reynolds et al. These include μ_{pe} (1/h), k_{npe} (mg/kg/h), λ_i (mg/kg), t_i (h), and δ (h) which are described in Table 1. However, all other equations and parameter values have been maintained to agree with those presented in Reynolds et al. A substantial number of these parameters were obtained from existing experimental literature (Table 1). For more information on parameter acquisition and estimation, please see the Supplementary Materials.

This model consists of a system of ordinary differential equations containing two pro-inflammatory mediators, N^* and D, as well as an anti-inflammatory mediator, C_A. N^* is biologically comparable to phagocytic immune cells or early, typically pro-inflammatory cytokines, such as *TNF* and *Interleukin-1* (*IL-1*). The other pro-inflammatory variable, D, not only serves as a marker for tissue damage/dysfunction, but also as a positive feedback into the earlier pro- and anti-inflammatory arms of the system, as damaged (e.g. injured or necrotic) tissue would (Matzinger, 2002). The anti-inflammatory mediator, C_A, acts on a slower time scale than N^*. For instance, C_A behaves more like the cytokine *Transforming Growth Factor-β1* (*TGF-β1*) rather than *Interleukin-10* (*IL-10*). However, it could also represent other typically anti-inflammatory mediators such as *cortisol*. In Section 4, we discuss the importance of dynamically modeling D and the necessity for the anti-inflammatory mediator to posses certain qualitative properties for tolerance to occur in the model.

Units for N^*, C_A, and D are not given explicitly because there is no single biological entity or marker that these variables represent and thus there are no specific units that can quantify these variables empirically. Hence, we use "N^*-units," "CA-units," and "D-units" because we cannot be any more precise about them. Although C_A (Anti-inflammatory Mediator) has characteristics of IL-10 and TGF-β, it would be inappropriate to assign real units to this variable and quantitatively compare it to actual data from these or other anti-inflammatory mediators.

Table 1
Model parameter names and values used in simulations

Name	Range	Value used	Description	Sources
μ_{pe}	0.6207–14.85	3/h	Decay rate of pathogen endotoxin (P_E)	(Iversen and Hahn, 1999; Warner et al., 1988; Yoshida et al., 1995)
λ_i	n/a	Various (mg/kg)	Amount of the ith P_E dose administration	
δ	n/a	0.01 or 24 h	Duration of P_E injection: 0.01 corresponds to instantaneous delivery (1/100 of an hour) and 24 corresponds to constant delivery of a dose over 24 h.	
t_i	n/a	Various (h)	Time at which the ith P_E dose is given	
k_{npe}	Estimated	9/(mg/kg)/h	Activation of phagocytes by pathogen endotoxin (P_E)	
k_{nn}	Estimated	0.01/N*-units/h	Activation of phagocytes by already activated phagocytes (or the cytokines that they produce)	
s_{nr}	Estimated	0.08 N_R-units/h	Source of resting phagocytes	
μ_{nr}	0.069-0.12	0.12/h	Decay rate of resting phagocytes (macrophages and neutrophils)	(Coxon et al., 1999)
μ_n	Less than μ_{nr}	0.05/h	Decay rate of activated phagocytes (macrophages and neutrophils)	(Coxon et al., 1999)
k_{nd}	Less than k_{npe}	0.02/D-units/h	Activation of phagocytes by tissue damage (D)	(Andersson et al., 2000)
k_{dn}	Estimated	0.35D-units/h	Max rate of damage production by activated phagocytes (and/or associated cytokines/free radicals)	
x_{dn}	Estimated	0.06 N*-units	Determines level of activated phagocytes (N*) needed to bring damage production up to half its maximum level	
μ_d	0.0174 (minimum)	0.02/h	Decay rate of damage; combination of repair, resolution, and regeneration of tissue HMGB-1 release by damage	(Degryse et al., 2001; Wang et al., 1999);
c_∞	Estimated	0.28 C_A-units	Threshold for effectiveness of the anti-inflammatory response	(Isler et al., 1999)
s_c	Estimated	0.0125 C_A-units/h	Source of anti-inflammatory (C_A) (IL-10, TGF-β1, cortisol);	
k_{cn}	Estimated	0.04 C_A-units/h	Maximum production rate of Anti-inflammatories	
k_{cnd}	Estimated	48 N*-units/D-units	Controls relative effectiveness of activated phagocytes versus damage in producing anti-inflammatories	
μ_c	0.15–2.19	0.1/h	Decay rate of C_A (il-10, cortisol, tnf-receptors and il-1 receptors)	(Bacon et al., 1973; Bocci, 1991; Fuchs et al., 1996; Huhn et al., 1997)

The immune response instigator, pathogen endotoxin or P_E (mg/kg), serves as the initial stimulus that recruits N* with a rate of k_{npe} which has units mg/kg/h. This begins the inflammatory cascade. P_E decays exponentially with rate μ_{pe}, having units per hour, with no other mediators affecting its decay. In addition, multiple intravenous injections (*i.v.*) of endotoxin can be emulated with Heaviside step functions in the P_E equation. The parameters λ_i and t_i in the Heaviside functions represent the endotoxin dosage load for dose i mg/kg given at time t_i hours, respectively, for $i = 1, 2, \ldots n$, the number of doses. If we want a total of λ mg/kg to be given over a duration of time, δ, then λ/δ (mg/kg/h) given for δ hours will accomplish this. The parameter δ is set to 0.01 h, which matches the time step of our numerical integration, when we wish to emulate a pulse, or a quick on–off, instantaneous injection. For instance, if $\delta = 0.01$, the administration of a load

amount of 3 mg/kg given at time t hours would stop at $t+\delta = t+0.01$ h, thereby essentially giving the whole load all at once. Larger values of δ will result in longer infusion times. For example, in scenario 8 we set δ equal to 24, thereby giving $3/24 = 0.125$ (mg/kg/h) continuously over the span of 24 h. This also gives a total of 3 mg/kg but over a longer span of time than the instantaneous injection. Although we model *i.v.* type injections, studies have shown that endotoxin administration given either intravenously or intraperitoneally invokes a similar inflammatory response (Copeland et al., 2005). Table 1 gives the parameter values that were established for this model, which is represented by Eqs. (1)–(4).

$$\frac{dP_E}{dt} = -\mu_{pe}P_E + \sum_{i=1}^{n} \frac{\lambda_i}{\delta} S(t_i, t_i + \delta), \tag{1}$$

$$\frac{dN^*}{dt} = \frac{s_{nr}R}{k_{nr} + R} - \mu_n N^*, \tag{2}$$

$$\frac{dD}{dt} = k_{dn}\frac{f(N^*)^6}{x_{dn}^6 + f(N^*)^6} - \mu_d D, \tag{3}$$

$$\frac{dC_A}{dt} = s_c + k_{cn}\frac{f(N^* + k_{cnd}D)}{1 + f(N^* + k_{cnd}D)} - \mu_c C_A, \tag{4}$$

where n is the number of doses in the experiment and the other functions in (1)–(4) are given by

$$R = \frac{(k_{npe}P_E + k_{nd}D + k_{nn}N^*)}{1 + (C_A/c_\infty)^2},$$

$$f(x) = \frac{x}{1 + (C_A/c_\infty)^2}$$

$$S(t_{on}, t_{off}) = H(t - t_{on}) - H(t - t_{off}),$$

$$= \begin{cases} 0 & \text{if } t < t_{on} \\ 1 & \text{if } t \geqslant t_{on} \end{cases} - \begin{cases} 0 & \text{if } t < t_{off}, \\ 1 & \text{if } t \geqslant t_{off}. \end{cases}$$

Using the parameter values given in Table 1, this system has three possible equilibrium states in the regime that we are interested in, namely where all solutions are non-negative. Two of the three fixed points are stable and the remaining one is a saddle whose stable manifold separates the phase space of interest into two regions, each containing one of the stable fixed points. One of the stable states is specified by the background levels of the variables, $(P_E, N^*, D, C_A) = (0,0,0,C_{A0})$. These low levels are characteristic of the state in which the system is at baseline, prior to any perturbation. Thus, when the mediators settle to this state we correspondingly interpret the outcome as healthy. The other stable equilibrium is classified as an unhealthy state in light of the fact that the values of the variables at this state are above background levels, except for P_E, which always decays asymptotically to zero. When the mediators are pulled to this state it indicates that the response has not properly resolved and, consequently, the outcome is unhealthy or inflamed.

The observations we make in our simulations have biological interpretations related to the characteristics of the acute inflammatory response. When we emulate an administration of endotoxin, the variables of the model react much like the mediators of the inflammatory response in the body in the presence of endotoxin, with their levels rising in the presence of this pro-inflammatory stimulus. After we induce this inflammatory response in our model with an injection of P_E, the system either settles to the healthy state or rises to the unhealthy state. If the dosage of P_E is large enough, it can elicit such a response that the system remains inflamed and is unable to return to its background levels. We equate such an outcome with persistent inflammation, which is an unhealthy endpoint. Given these features of our system, we interpret the existence of endotoxin tolerance in our model as a reduction in the response of N^* to a low dose of P_E after the system is preconditioned with an initial low P_E dose.

Likewise, if a preconditioning dose of P_E prevents the system from ending up at the unhealthy state when an otherwise unhealthy dose is given, we infer this as the ability of the model to display protection from mortality. Using the model Eqs. (1)–(4), with parameter values from Tables 1 and 7, we are able to qualitatively reproduce the results of various published scenarios of repeated endotoxin administration, which we now discuss.

3. Model simulations of experimental scenarios

For our in silico simulations, we emulate the scenarios below using the dynamical systems analysis software XPPAUT (Ermentrout, 2002). Eqs. (1)–(4) are integrated numerically using the Runge–Kutta algorithm with step size 0.01 for 200 time units (hours), taking into account the simulated *i.v.* injections of P_E at the specified times. Thus, the design of our in silico endotoxin simulations can closely resemble actual endotoxin experimental scenarios, which originally were carried out with mice. The XPPAUT code for this model is included with the Supplementary Materials.

We start with the reproduction of proper responses to survivable and lethal endotoxin doses, simulated by simply varying the load (λ_1 mg/kg) of P_E at time zero ($t_1 = 0$ h). Regarding endotoxin administration and mortality, it is generally accepted that doses at or above 17 mg/kg cause a high mortality rate in mice (National Research Council, 1992). Figs. 1a and b show the results of the model simulations carried out with low (Fig. 1a) and high (Fig. 1b) P_E doses. Having established these basic responses, we now consider experiments involving repeated endotoxin administration, most of which are based on experimental data in the literature.

3.1. Endotoxin tolerance scenarios

Published studies report that endotoxin tolerance can be induced in various ways, generally involving the administration of low, repeated doses of endotoxin over periods of time ranging from one day to a week (Balkhy and Heinzel, 1999; Berg et al., 1995; Rayhane et al., 1999; Sly et al., 2004; Wysocka et al., 2001). Blood serum is collected at some time after the last (challenge) endotoxin dose, and inflammatory analytes (generally *TNF*) are measured. In all the above cited experiments, a reduced amount of *TNF* is seen in the group receiving more than one dose of endotoxin (preconditioned) as compared to the amount of *TNF* found in the serum of mice receiving only a single dose of endotoxin (non-preconditioned).

Scenarios 1–5 closely follow various experimental scenarios of repeated endotoxin administration as they are outlined in the literature. Tables 2–6 summarize the designs and results of these scenarios which are reproduced in our model simulations with respect to a qualitative reduction in our pro-inflammatory mediators, specifically N^*. Scenarios 6–8 are not explicitly found in the literature,
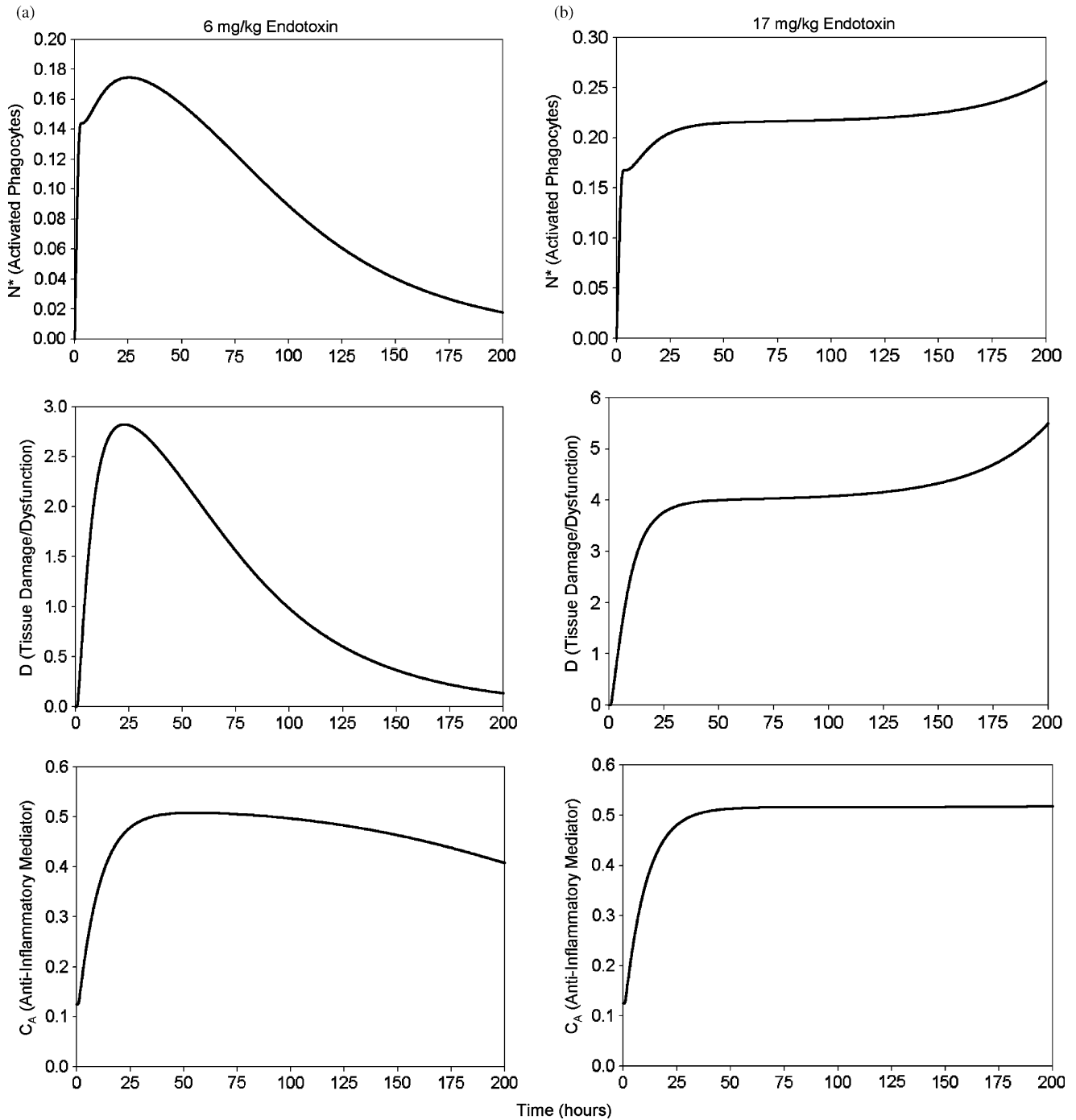
(a)

(b)

Fig. 1. Basic endotoxin administration scenarios. The values of the parameters λ_1, t_1, and δ are set to simulate a one dose instantaneous ($\delta = .01$) administration of P_E at time zero ($t_1 = 0$). (a) Doses less than $\lambda_1 = 17$ mg/kg of P_E cause a response, but all mediators eventually settle back to baseline in a healthy resolution. Here we show a simulation done with a dose of $\lambda_1 = 6$ mg/kg of P_E. (b) Doses greater than or equal to $\lambda_1 = 17$ mg/kg of P_E cause all mediators to remain elevated, indicating an unhealthy outcome. The simulation results shown are carried out with a dose of $\lambda_1 = 17$ mg/kg of P_E. Time courses for N^*, D, and C_A are shown for both scenarios.

Table 2
Scenario 1 (adapted from the experiments of Sly et al., 2004)

Sly et al. (2004)	0 h	24 h	Experimental results
Non-preconditioned	Saline	10 mg/kg	600 pg/ml TNF at 27 h
Preconditioned	1 mg/kg	10 mg/kg	TNF levels very low at 27 h

yet we believe them to be relevant scenarios that merit consideration. The parameter values appearing in Table 1 are used for all the scenarios discussed in this section, with the exception of parameters that are used to set up *i.v.* P_E administrations for the various simulations: λ_i, t_i, and δ. The values for these parameters as pertains to the different scenarios can be found in Table 7.

Scenario 1 is based on the experiments of Sly and colleagues (2004), summarized in Table 2. Fig. 2a, c and d show the time courses for the model variables obtained for this first scenario and Fig. 2b is a bar graph of selected time points from the numerical data shown in Fig. 2a. Scenario 2 follows the endotoxin tolerance experiments of Wysocka et al. (2001), outlined in Table 3, where tolerance is induced with a variety of preconditioning doses ranging from 0.05 to 1 mg/kg. A qualitative reproduction of their results by our model can be seen in the time courses of Fig. 3. It is interesting to note that the preconditioning dose used in scenario 2b allows for the greatest reduction in N^* compared to doses used for scenarios 2a and 2c. This indicates that for a fixed preconditioning time interval, the size of the preconditioning dose can determine the magnitude of the reduction that is detected, with a non-monotonic relationship between the two. We address this observation in more detail in Section 5.

Scenario 3 is based on the experiments done by Rayhane et al. (1999). Two of these experiments are more complicated than those of Sly et al. and Wysocka et al., since several preconditioning doses, rather than only one, are given before the challenging dose. In Table 4, the designs of the three separate tolerance experiments from Rayhane et al. are outlined along with a summary of their results. Fig. 4 shows our results.

The experiment of Balkhy and Heinzel (1999), scenario 4 outlined in Table 5, is slightly different from the previous scenarios we have simulated, in that the final endotoxin dose (15 mg/kg) is given 48 h after the last preconditioning dose, instead of only 24 or 26 h after. Fig. 5 shows the results of our simulations for this scenario. We note that if we had simulated giving the challenge dose of 15 mg/kg earlier than 48 h after preconditioning (e.g. at 24 or 26 h after), this regimen would have led the system to the unhealthy state. This finding highlights the importance of timing as well as dosage size to tolerance outcomes.

Table 3
Scenarios 2a–2c (adapted from the experiment of Wysocka et al., 2001)

Wysocka et al. (2001)	0 h	26 h	Experimental results
Non-preconditioned	Saline	100 mcg	100 ng/ml TNF at 27 h
Preconditioned 2a	1 mcg	100 mcg	<20 ng/ml TNF at 27 h
Preconditioned 2b	5 mcg	100 mcg	<20 ng/ml TNF at 27 h
Preconditioned 2c	20 mcg	100 mcg	<20 ng/ml TNF at 27 h

Mouse weight is estimated at 20 g: 1 mcg/mouse = 0.05 mg/kg, 5 mcg/mouse = 0.25 mg/kg, 20 mcg/mouse = 1.0 mg/kg, and 100 mcg/mouse = 5.0 mg/kg.

Table 6
Scenario 5 (adapted from the experiments of Berg et al., 1995)

Berg et al. (1995)	0 h	24 h	Experimental results
Non-preconditioned	Saline	200 mcg	No mice survived
Preconditioned	25 mcg	200 mcg	All mice survived

Mouse weight is estimated at 20 g: 25 mcg/mouse = 1.25 mg/kg and 200 mcg/mouse = 10 mg/kg.

Table 4
Scenarios 3a–3c (adapted from the experiments of Rayhane et al., 1999)

Rayhane et al. (1999)	0 h	24 h	48 h	72 h	Experimental results
Non- preconditioned 3a	Saline	100 mcg	n/a	n/a	35 ng/ml TNF (at 25.5 h); 2.5 ng/ml TNF (at 27 h)
Preconditioned 3a	2.5 mcg	100 mcg	n/a	n/a	3 ng/ml TNF (at 25.5 h); 2 ng/ml TNF (at 27 h)
Non-preconditioned 3b	Saline	Saline	100 mcg	n/a	35 ng/ml TNF (at 49.5 h); 2.5 ng/ml TNF (at 51 h)
Preconditioned 3b	2.5 mcg	2.5 mcg	100 mcg	n/a	1 ng/ml TNF (at 49.5 h); .5 ng/ml TNF (at 51 h)
Non-preconditioned 3c	Saline	Saline	Saline	100 mcg	35 ng/ml TNF (at 73.5 h); 2.5 ng/ml TNF (at 75 h)
Preconditioned 3c	2.5 mcg	2.5 mcg	2.5 mcg	100 mcg	1 ng/ml TNF (at 73.5 h); .5 ng/ml TNF (at 75 h)

Mouse weight is estimated at 20 g: 2.5 mcg/mouse = 0.125 mg/kg and 100 mcg/mouse = 5.0 mg/kg.

Table 5
Scenario 4 (adapted from the experiments of Balkhy and Heinzel, 1999)

Balkhy and Heinzel (1999)	0 h	24 h	48 h	72 h	Experimental results
Non-preconditioned	Saline	Saline	n/a	300 mcg	
Preconditioned	50 mcg	50 mcg	n/a	300 mcg	3- to 6-fold reduction in the peak serum TNF-α levels at 73 h

Mouse weight is estimated at 20 g: 50 mcg/mouse = 2.5 mg/kg and 300 mcg/mouse = 15 mg/kg.

Table 7
Endotoxin administration parameter values and figure references for in silico simulations of Scenarios 1–8

	λ_1 (mg/kg)	t_1 (h)	λ_2 (mg/kg)	t_2 (h)	λ_3 (mg/kg)	t_3 (h)	λ_4 (mg/kg)	t_4 (h)	δ (h)	Figure references
Scenario 1										2a–2d
Non-preconditioned	0.0	0	10.0	24	n/a	n/a	n/a	n/a	0.01	
Preconditioned	1.0	0	10.0	24	n/a	n/a	n/a	n/a	0.01	
Scenarios 2a–2c										3a–3c
Non-preconditioned	0.0	0	5.0	26	n/a	n/a	n/a	n/a	0.01	
Preconditioned 2a	0.05	0	5.0	26	n/a	n/a	n/a	n/a	0.01	
Preconditioned 2b	0.25	0	5.0	26	n/a	n/a	n/a	n/a	0.01	
Preconditioned 2c	1.0	0	5.0	26	n/a	n/a	n/a	n/a	0.01	
Scenarios 3a–3c										4a–4c
Non-preconditioned 3a	0.0	0	5.0	24	n/a	n/a	n/a	n/a	0.01	
Preconditioned 3a	0.125	0	5.0	24	n/a	n/a	n/a	n/a	0.01	
Non-preconditioned 3b	0.0	0	0.0	24	5.0	48	n/a	n/a	0.01	
Preconditioned 3b	0.125	0	0.125	24	5.0	48	n/a	n/a	0.01	
Non-preconditioned 3c	0.0	0	0.0	24	0.0	48	5.0	72	0.01	
Preconditioned 3c	0.125	0	0.125	24	0.125	48	5.0	72	0.01	
Scenario 4										5
Non-Preconditioned	0.0	0	0.0	24	15.0	72	n/a	n/a	0.01	
Preconditioned 4a	2.5	0	2.5	24	15.0	72	n/a	n/a	0.01	
Preconditioned 4b	0.125	0	0.125	24	0.125	48	5.0	72	0.01	
Scenario 5										6a–6b
Non-preconditioned	0.0	0	17.0	24	n/a	n/a	n/a	n/a	0.01	
Preconditioned	1.25	0	17.0	24	n/a	n/a	n/a	n/a	0.01	
Scenario 6										7a–7b
Non-preconditioned	0.0	0	6.0	24	n/a	n/a	n/a	n/a	0.01	
Preconditioned	3.0	0	6.0	24	n/a	n/a	n/a	n/a	0.01	
Scenario 7										8a–8b
Non-preconditioned	0.0	0	6.0	15	n/a	n/a	n/a	n/a	0.01	
Preconditioned	3.0	0	6.0	15	n/a	n/a	n/a	n/a	0.01	
Scenario 8										9a–9d
Instantaneous injection	3.0	0	n/a	n/a	n/a	n/a	n/a	n/a	0.01	
Continuous infusion	3.0	0	n/a	n/a	n/a	n/a	n/a	n/a	24.0	

Scenarios 1–5 are based on those found in Tables 2–6. As an example, parameters for one simulation may be set as follows: $t_1 = 0$ h, $\lambda_1 = 0$ mg/kg, $t_2 = 24$ h, $\lambda_2 = 10$ mg/kg, and $\delta = .01$ h. This is analogous to giving a saline (non-preconditioned) dose ($\lambda_1 = 0$ mg/kg) to mice at time zero ($t_1 = 0$ h) and then giving a second dose ($\lambda_2 = 10$ mg/kg) of endotoxin at 24 h ($t_2 = 24$ h) with both doses given as instantaneous injections ($\delta = 0.01$ h) at the specified times. The system is then integrated and one can look at time courses of the model variables. These parameters can be changed and the system integrated again to give another set of time courses for comparison.

As mentioned previously, endotoxin, when given above a certain threshold dose, can be lethal for mice. This threshold can depend on specific experimental conditions as well as the strain of mouse used. However, experiments have shown that preconditioning mice with a low, survivable P_E dose can actually prevent animals from succumbing to a lethal challenge dose (Berg et al., 1995; Sly et al., 2004; Yadavalli et al., 2001). We conduct a model simulation of this effect using the experiment of Berg et al. (1995) as a guideline (Scenario 5, Table 6). A dose of 10 mg/kg proved to be lethal in the mice that were used in Berg's experiment; however, based on our own studies, the lethal dose in our model is centered at 17 mg/kg (Chow et al., 2005). Thus, our potentially lethal challenge dose in our simulations is $\lambda_1 = 17$ mg/kg of P_E. Figs. 6a and b show the simulation time courses for N^* and D, respectively, where we see that preconditioning enables a rescue from an otherwise lethal insult.

3.2. Potentiation scenarios: sub-lethal and lethal doses

Experimentally, when the time between initial exposure to endotoxin and the secondary challenge is short relative to the magnitude of the endotoxin doses, an increase, rather than a reduction, of inflammation (i.e. *TNF*) is observed upon repeated endotoxin administrations. This phenomenon is referred to as potentiation (Cavaillon, 1995). As we will discuss in further detail later, both the timing of the administration of the doses as well as their magnitudes determine the final outcome of tolerance or potentiation. The scenarios introduced in this section demonstrate potentiation in several different forms.

Scenarios 6 and 7 which are not explicitly based on experiments found in the literature demonstrate sub-lethal and lethal potentiation simulations, respectively. Figs. 7a and b show that in scenario 6 there is a clear elevation in the amount of N^* in the preconditioned simulation,
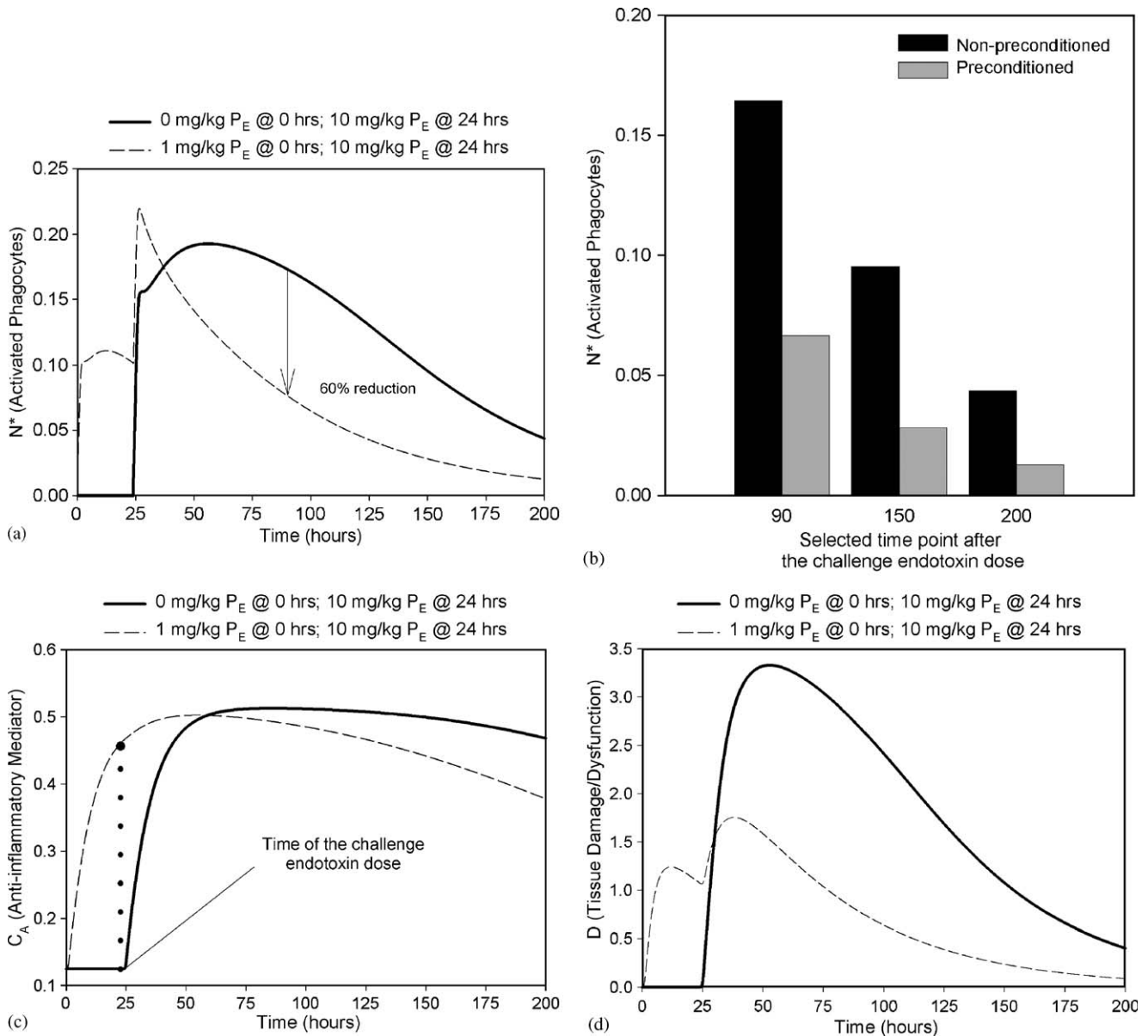
Fig. 2. Numerical results of simulations following scenario 1 in Table 2, with administration parameters set as in Table 7 for Scenario 1. (a) Time courses of N^* for the non-preconditioned (solid) and preconditioned simulations (dashed), showing a maximum reduction of 60% as indicated by the downward arrow. In actual experiments, the data cannot usually be viewed as continuous time course curves. Instead, bar graphs are given showing the amount of certain analytes at a specified time after the challenge endotoxin administration, comparing the non-preconditioned group to the preconditioned group. To relate our in silico results to this convention, (b) shows a bar graph of the amount of N^* in both the non-preconditioned and preconditioned simulations at several time points after the challenge endotoxin administration, where a reduction in N^* is seen. (c)–(d) Time courses of C_A and D, respectively, for the non-preconditioned (solid curve) and preconditioned simulations (dashed curve). The dotted vertical line in (c) denotes the time the challenge P_E dose was given.

compared to that of the non-preconditioned one, but the mediators eventually resolve to the healthy state. In scenario 7, Figs. 8a and b show that the non-preconditioned simulation results in a healthy outcome whereas the preconditioned one results in an unhealthy outcome. Comparing Scenarios 6 and 7 show that the timing and not just the amount of the second endotoxin dose determines whether or not the potentiation leads to an increase in N^* that eventually settles back to the healthy equilibrium, or to an increase that converges to the unhealthy state.

In order to experimentally simulate the kinetics of endotoxin release in animals during sepsis, a continuous, low-dose infusion of endotoxin is administered (Parker and Watkins, 2001). Scenario 8 demonstrates that gradually administering a dose of $3 \text{ mg/kg } P_E$ over 24 h forces the system to the unhealthy state, whereas the same dose given as an abrupt bolus does not. To approximate the instantaneous administration of $3 \text{ mg/kg } P_E$ into the system, we set $t_1 = 0$, $\lambda_1 = 3$, and $\delta = 0.01$ (Fig. 9a). To simulate $3 \text{ mg/kg } P_E$ given over 24 h at a constant rate, we set $\delta = 24$. In setting δ to a value of 24 we are simulating an
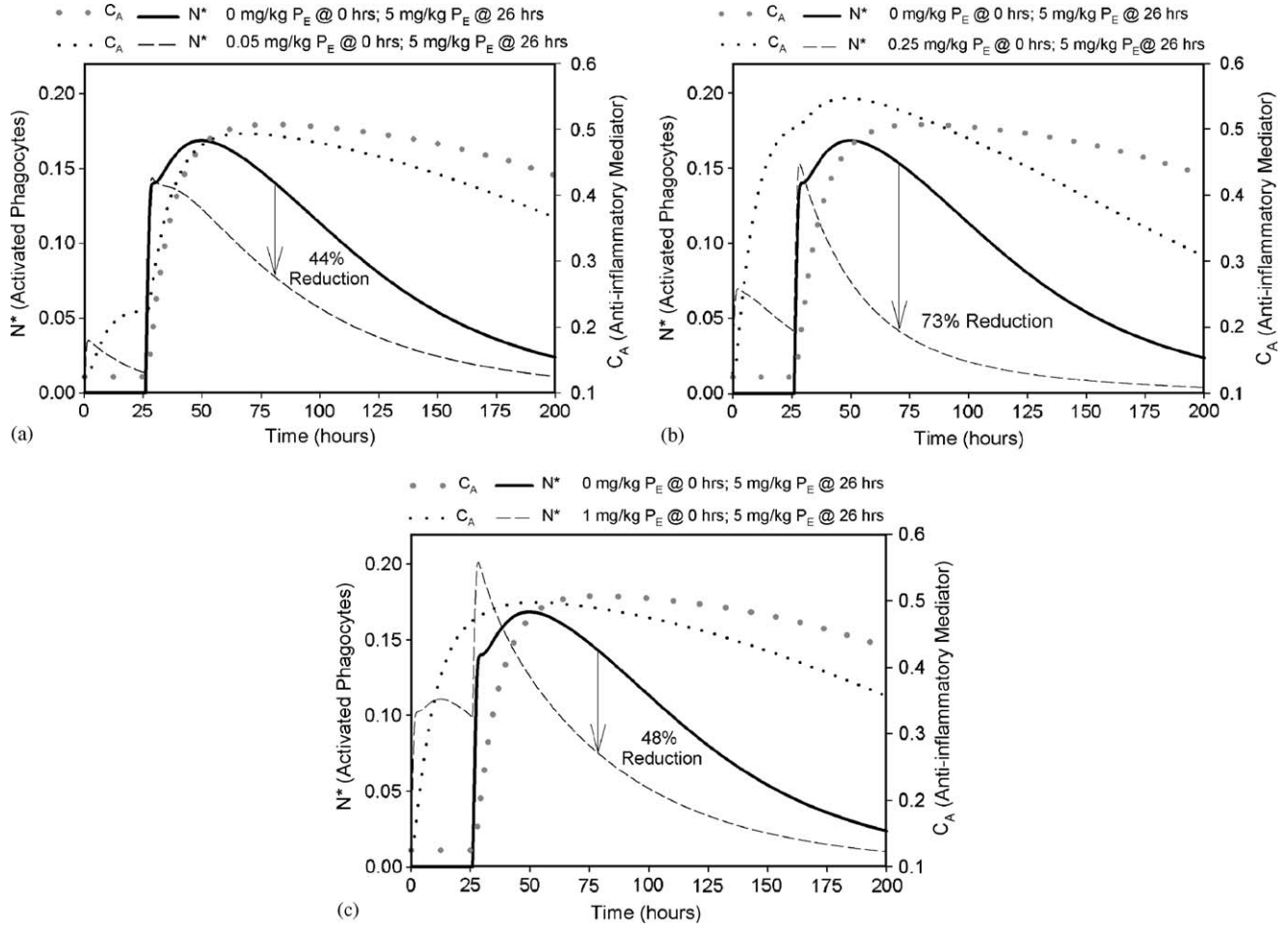
Fig. 3. Numerical results of simulations following scenarios 2a–2c in Table 3, with dosage amounts converted from micrograms/mouse to milligrams/kilogram in order to conform to the units of P_E (mg/kg) in our model. Administration parameters are set as in Table 7 for scenarios 2a–2c. Time courses of N^* for the non-preconditioned (solid) and preconditioned simulations (dashed) are shown for each scenario. Compared to the non-preconditioned simulation, there is a maximum reduction in N^* of 44% in (a) scenario 2a, 73% in (b) scenario 2b and 48% in (c) scenario 2c, indicated in each figure by the downward arrows. The time courses of C_A, for the non-preconditioned (large dots) and preconditioned (small dots) simulations, are also shown on each graph with a separate axis on the right of each graph.

endotoxin infusion that distributes a total of 3 mg/kg P_E gradually over 24 h (Fig. 9b). This is a fair comparison, because in both cases, in the absence of decay of P_E, the P_E level at the end of the infusion would be 3 mg/kg. Figs. 9c and d show that the constant administration of P_E, even though it is administered in very low amounts, causes the system to converge to the unhealthy state, whereas the instantaneous dose does not. These results imply that insults that elicit a strong initial pro-inflammatory response properly counter-balanced by an anti-inflammatory response are more likely to be tolerated by the host. In contrast, those stimuli that cause an initially weak but persistent response can be detrimental to the host.

4. The importance of the dynamics of the late pro-inflammatory and anti-inflammatory mediators to tolerance

A system of ordinary differential equations becomes complicated very rapidly as the number of equations increases. It can, therefore, be advantageous to attempt to reduce the number of equations to a manageable number by applying a *steady state assumption*. This strategy is most appropriately applied to variables that are transient, and is accomplished by setting their derivatives to zero; for example, if $x' = f(x, y)$, then we apply the steady state assumption to x by setting $x = X(y)$ such that $f(X(y), y) = 0$, if such an $X(y)$ exists. By making such a substitution, one is assuming that the relevant variable reaches its steady state quickly and does not deviate from it over time, although the particular value of its steady state may vary as the other quantities in the system evolve. Based on the form of the model in Section 2, it would be most convenient to reduce the number of equations in our model by applying the steady state assumption to D, although in fact it behaves as a slow-acting pro-inflammatory mediator. As it turns out, under the steady state assumption on D, the model fails to reproduce the experimentally observed endotoxin tolerance results without parameter modifications that compromise the basic model performance or are outside of the physiologic range.
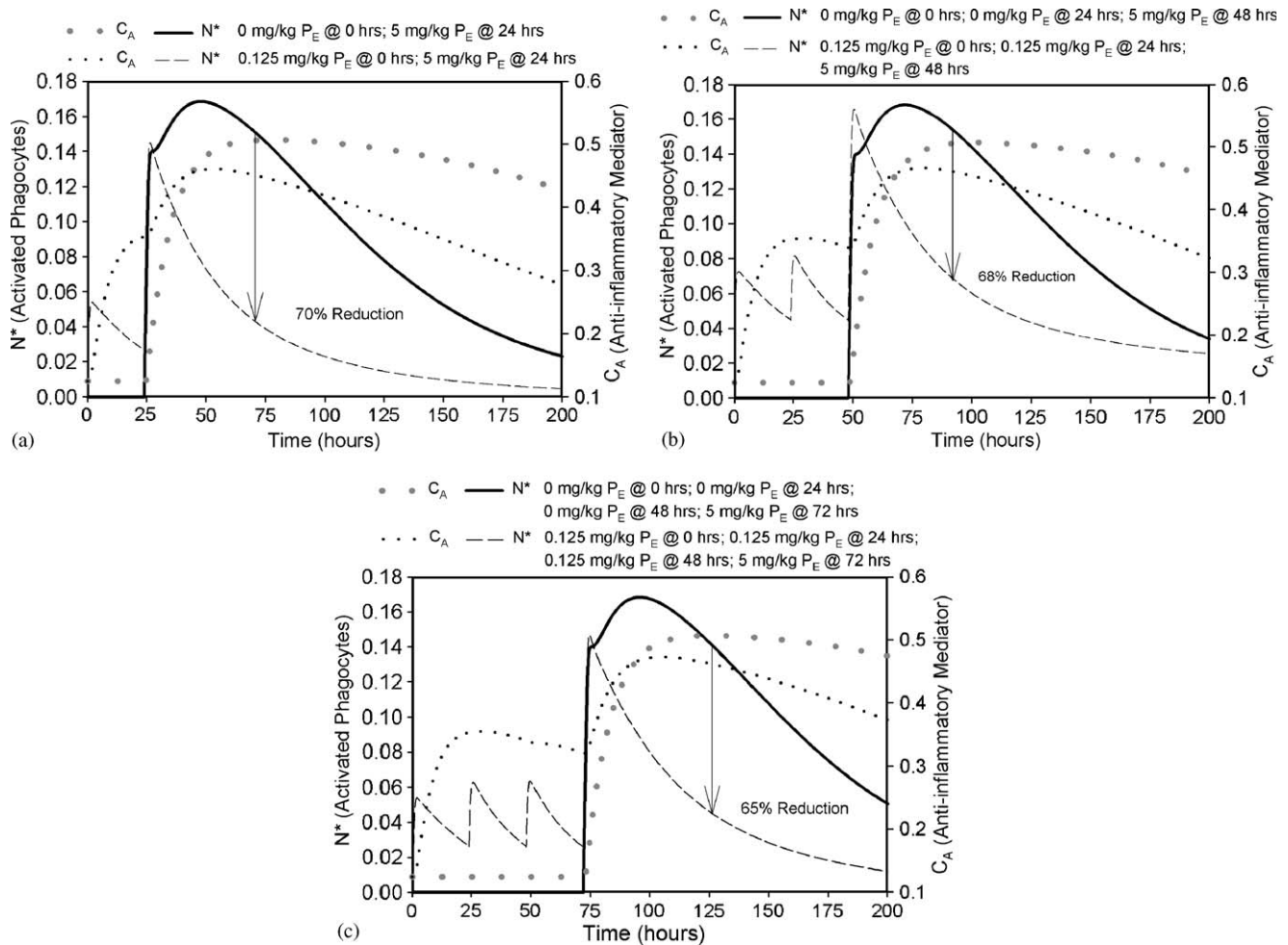
Fig. 4. Numerical results of simulations following scenarios 3a–3c in Table 4, with dosage amounts converted from micrograms/mouse to milligrams/kilogram in order to conform to the units of P_E (mg/kg) in our model. Model parameters are set as in Table 7 for Scenarios 3a–3c. Time courses of N^* for the non-preconditioned (solid) and preconditioned simulations (dashed) are shown for each scenario. Measured against the non-preconditioned simulations, we see a reduction in N^* of 70% in (a) scenario 3a, 68% in (b) scenario 3b, and 65% in (c) scenario 3c, indicated in each figure by the downward arrows. The time courses of C_A, for the non-preconditioned (large dots) and preconditioned (small dots) simulations, are also shown on each graph with a separate axis on the right of each graph.

As mentioned, we define the existence of endotoxin tolerance in our model as a reduced N^* response to a low dose of P_E when the system is preconditioned with an initial low P_E dose. However, with D in steady state, we observe only potentiation of the N^* response regardless of when the second dose is administered. On the other hand, parameters can be changed to achieve tolerance, but these changes eliminate the possibility for the system to reach an unhealthy state, which is necessary in order for the model to retain basic biological fidelity. As previously mentioned, experiments have verified that a low preconditioning dose of endotoxin can rescue mice from a normally lethal endotoxin dose (Rayhane et al., 1999; Sly et al., 2004; Yadavalli et al., 2001). However, with D in steady state, a lethal P_E dose always leads to an unhealthy state even after a low preconditioning dose of P_E is given and, in fact, does so more prominently when the system is preconditioned.

Thus, dynamically modeling D allows for a number of outcomes that are not possible otherwise within the bounds

of the biological constraints imposed by past experimental findings. The fact that D acts gradually and promotes the production of C_A allows the model to attain an extended C_A elevation, without compromising the existence of an unhealthy state in the system. This attribute of our model plays an important role in the reproduction of tolerance scenarios. We explored this further by looking at the effects that certain forms of altered C_A dynamics had on tolerance in our model (with dynamic D). First, appropriate model parameter values were adjusted so that C_A was only being produced by early immune responders (N^*) and so that it had an early peak and a relatively quick decay. The time course of C_A then closely resembled that of a fast acting anti-inflammatory cytokine, such as IL-10. In this scenario, the regimes of healthy and unhealthy still exist; however, tolerance does not occur. Indeed, preconditioning led to potentiation of the N^* response and sometimes caused the otherwise sub-lethal challenge dose to be lethal, much like what happened when D was assumed to be in steady state.
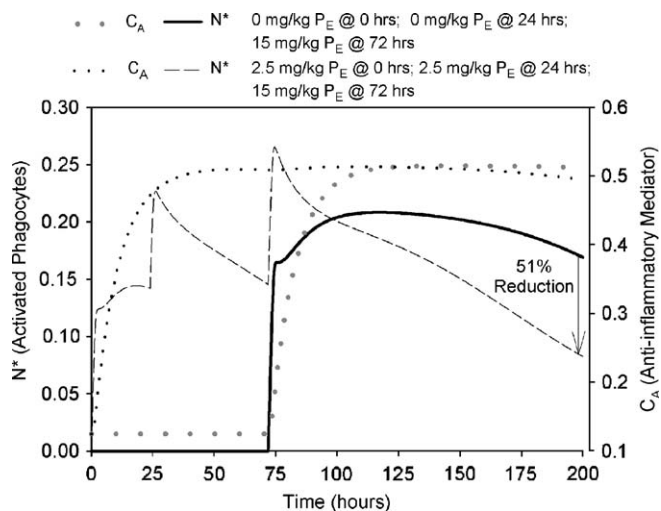
Fig. 5. Numerical results of simulations following scenario 4 in Table 5, with model parameters set as in Table 7 for scenario 4. Time courses of N^* are shown for the non-preconditioned (solid) and the preconditioned simulations (dashed). Balkhy and Heinzel report a 3- to 6-fold reduction of serum TNF one hour after the challenge dose is given, compared to non-preconditioned results. Although our model does not capture an immediate reduction in our pro-inflammatory mediator, N^*, we do observe a significant reduction overall, as seen in this figure. The time courses of C_A, for the non-preconditioned (large dots) and preconditioned (small dots) simulations, are also shown with a separate axis on the right of the graph.

Therefore, it appears that for tolerance to occur in our model, C_A cannot solely behave as an early anti-inflammatory mediator, like IL-10.

On the other hand, another possible modification was to adjust model parameters so that C_A behaved as a later acting anti-inflammatory, accumulating on a time scale comparable to that of D. We found that significant changes in this direction drastically shrank the basin of attraction[1] of the healthy state. In some ways, modifying C_A in this way is comparable to considering IL-10-deficient (knock-out) mice, and indeed a similar sensitivity to small endotoxin doses is seen experimentally in these animals (Berg et al., 1995; Wysocka et al., 2001). Tolerance effects have been seen in experiments with IL-10 knockout mice. It is likely, however, that such knockout mice have a decreased susceptibility to pro-inflammatory stimuli or an increased upregulation of other anti-inflammatory mediators to compensate for the absence of IL-10 early on in the immune response, which our model does not incorporate. Indeed, simulation of our model suggests that removal of early anti-inflammatory mediators without compensation would eliminate tolerance, since endotoxin doses small enough to be sub-lethal, given the decreased basin of attraction of the healthy state, fail to activate C_A sufficiently for tolerance to occur.

---

[1]The *basin of attraction* of a stable fixed point, x^*, of a dynamical system is the set of all initial conditions that dynamically evolve to x^* (Strogatz, 1994; Weisstein, 2006).
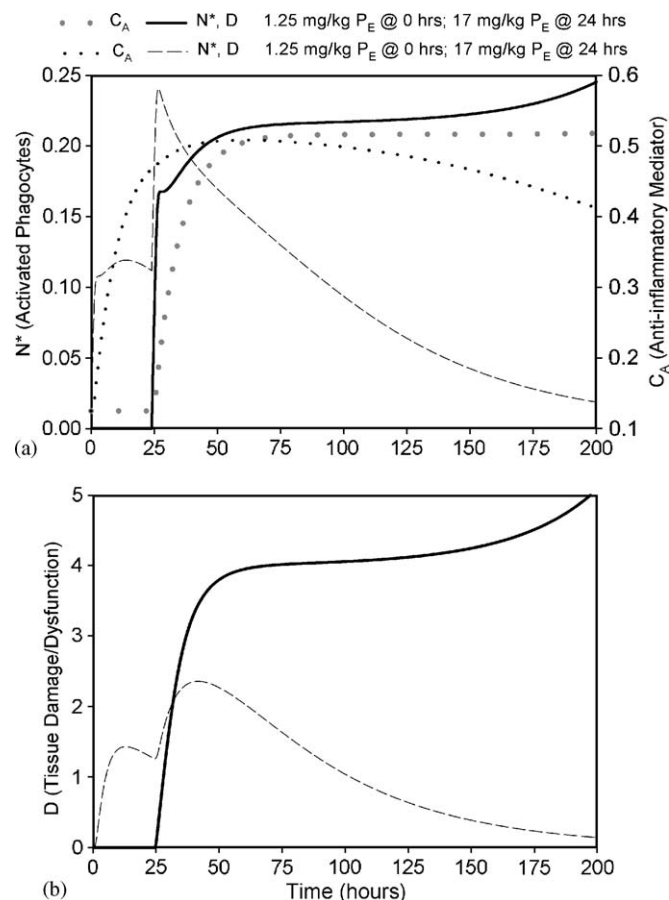

Fig. 6. Numerical results of simulations based on scenario 5 in Table 6, with model parameters set as in Table 7 for scenario 5. This scenario demonstrates that our model qualitatively captures the result that a small preconditioning dose of endotoxin can prevent the negative outcome of an otherwise lethal dose. (a)–(b) Time courses of N^* and D, respectively, for the non-preconditioned (solid) and preconditioned simulations (dashed). The time courses of C_A, for the non-preconditioned (large dots) and preconditioned (small dots) simulations, are also shown on the N^* graph with a separate axis on the right of the graph. The non-preconditioned simulation clearly ends up at the unhealthy state, in which N^* and D remain high. However, the simulation that was preconditioned settles to the low healthy state, showing rescue from an otherwise lethal insult.

5. Insight from the model's responses to endotoxin administration

Looking at these preconditioning phenomena from the point of view of the dynamics of a mathematical model of the acute inflammatory response, we are able to offer insight into why these disparate results are seen experimentally. It is important to note that the development of this model only took into account empirical observations about the interactions of somewhat abstracted immune effectors. However, none of the endotoxin administration results that we have reproduced was built into the development of the equations. Rather, our findings emerge from the interactions of the dynamic variables and biological effects of repeated endotoxin administration. Thus, although *petitio principii* or "circular reasoning" is a
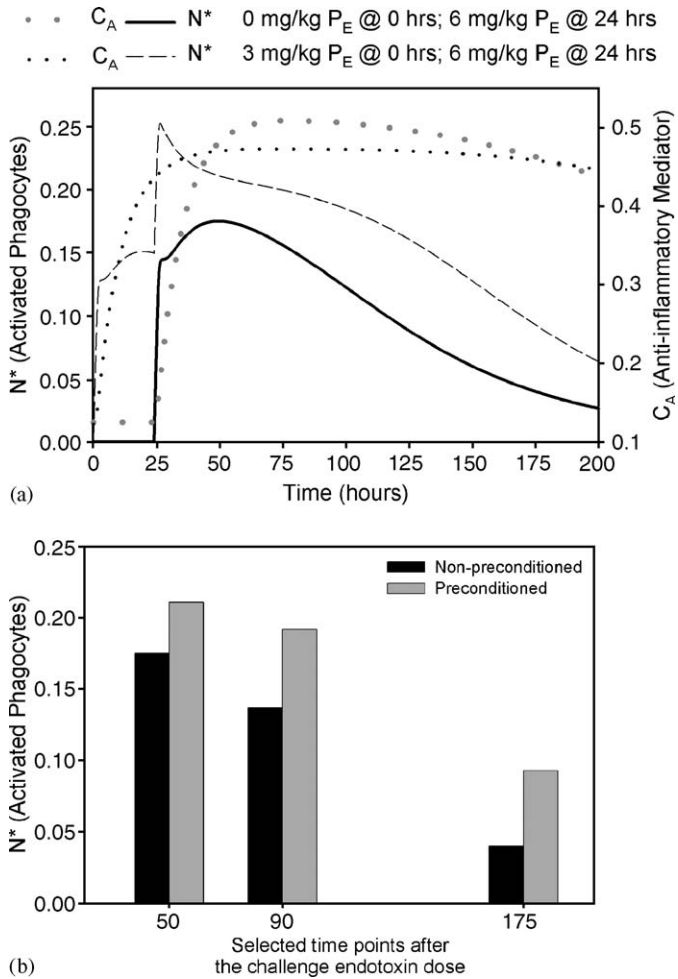
Fig. 7. Numerical results of simulations for sub-lethal potentiation scenario. (a) Time courses of N^* for the non-preconditioned (solid) and preconditioned simulations (dashed), showing an increase in the amount of N^* with preconditioning compared to the non-preconditioned simulation. The time courses of C_A, for the non-preconditioned (large dots) and preconditioned (small dots) simulations, are also shown on the N^* graph with a separate axis on the right of the graph. (b) Bar graph of selected time points from (7a), showing the amount of increase in N^*.

Fig. 8. Numerical results of simulations for lethal potentiation scenario. (a)–(b) Time courses of N^* and D, respectively, for the non-preconditioned (solid) and preconditioned simulations (dashed). The time courses of, C_A, for the non-preconditioned (large dots) and preconditioned (small dots) simulations are also shown on the N^* graph with a separate axis on the right of the graph. Unlike the non-preconditioned simulation, the preconditioned simulation results in an unhealthy response.

potential pitfall of such reduced models, the model we present was not constructed to describe the specific paradigm of endotoxin tolerance.

The timing and magnitude of the endotoxin doses plays a crucial role in the types of outcomes that are observed. In the model considered, the variable N^* is inhibited by C_A, the levels of which can remain elevated even after enough time has passed for N^* to start returning to its resting value. Using scenario 1 as an example, Fig. 2c demonstrates how the amount of C_A varies between the non-preconditioned and preconditioned simulations at the time that the second P_E dose is given (dotted vertical line). Comparing the amount of the anti-inflammatory mediator in the two simulations at this time point, we see that with preconditioning there are significantly higher levels of C_A than without preconditioning, which shows C_A levels that are still at baseline. In scenarios 1–4, which lead to
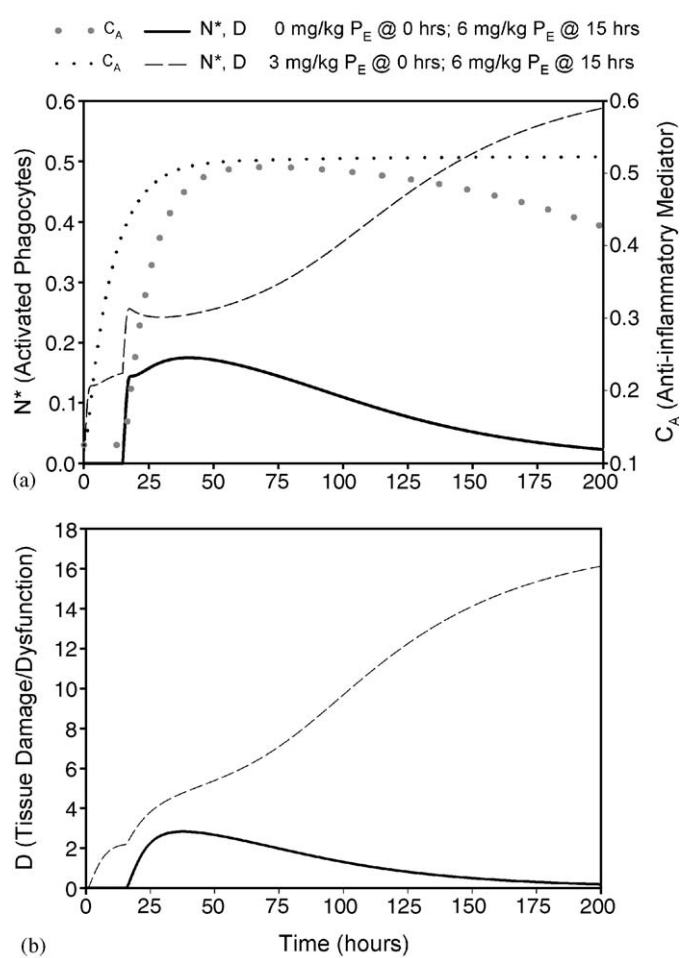
endotoxin tolerance, the challenge endotoxin dose that follows the preconditioning regimen is given during a time when the system is precisely in this state of relatively low N^* and elevated C_A. The build-up of the anti-inflammatory mediator, induced by preconditioning, results in a reduction of the overall inflammation or build-up of N^*, incited by the challenge endotoxin dose. Fig. 2c also shows that even though a short time after the challenge dose the levels of the anti-inflammatory mediator for the non-preconditioned simulation have risen above the preconditioned simulation levels, this occurs too long after the final endotoxin stimulus to influence the relative levels of N^* across the two experiments.

It is important to note that, despite the inhibitory effects of C_A, the full model exhibits an attracting, unhealthy steady state that can be attained, for example, following the introduction of a single, sufficiently large dose of endotoxin.
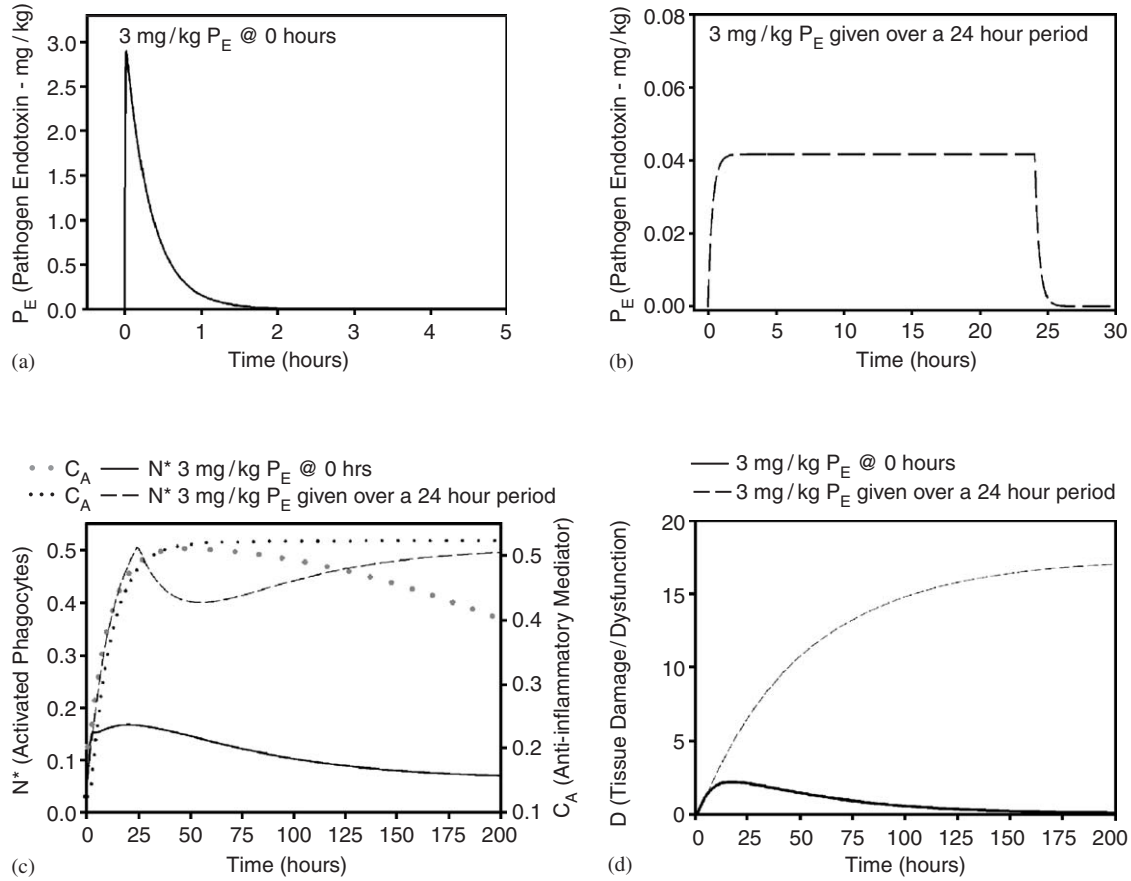
Fig. 9. Instantaneous versus continuous P_E administration. (a) Time course of P_E for the simulation giving an instantaneous injection of 3 mg/kg P_E into the system. (b) Time course of P_E for the simulation giving 3 mg/kg P_E over 24 h at a constant rate. This is done by setting $\delta = 24$ in the P_E equation. In setting δ to a value of 24 we are simulating an endotoxin *infusion* that distributes a total of 3 mg/kg P_E over 24 h rather than an instantaneous introduction of that amount. (c)–(d) Time courses of N^* and D, respectively, for the instantaneous administration simulation (solid) and continuous administration simulation (dashed) time courses. The time courses of C_A, for the instantaneous administration (large dots) and continuous administration (small dots) simulations, are also shown on the N^* graph with a separate axis on the right of the graph.

For the rescue phenomenon demonstrated in scenario 5 (Figs. 6a and b), we see that a preconditioning dose of endotoxin can prevent the system from reaching the unhealthy state upon subsequent exposure to an otherwise lethal endotoxin dose. Such a rescue is possible because the preconditioning changes the state in which the system lies when the lethal dose is encountered. Specifically, the anti-inflammatory mediator rises enough and the pro-inflammatory mediators are close enough to equilibrium after the preconditioning dose so that when the previously lethal endotoxin stimulus is given, the system lies in the basin of attraction of the healthy, baseline state, rather than that of the unhealthy state.

This behavior is similar to the tolerance observed in scenarios 1–4. The results from scenario 1 (Figs. 2a and c) are utilized in Figs. 10b and c to illustrate this by showing a projection of the system onto the N^*-C_A phase plane where trajectories for N^* and C_A can be seen with respect to their nullclines ($dN^*/dt = 0$ and $dC_A/dt = 0$).[2] For comparison,

related time courses of N^* are shown in Fig. 10a. In addition to the elevation of C_A above equilibrium when the challenge endotoxin dose is administered, the proximity of N^* and D to their equilibrium levels is equally important for both tolerance and rescue to occur, since the (N^*,D) subsystem forms a positive feedback loop. As long as the level of N^* or D remains too high, the introduction of the lethal endotoxin dose will place the system in the basin of attraction of the unhealthy state. The potentiation phenomenon illustrated in scenario 6 (Fig. 7a) follows similarly, stemming from a second endotoxin dose that comes soon after the initial one. Figs. 11a–c use the same strategy demonstrated with Figs. 10a–c this time using the results of scenario 6 to illustrate potentiation from the

---

[2] For a planar system $dx/dt = f(x, y)$, $dy/dt = g(x, y)$, the *nullclines* are the two curves $f = 0$ and $g = 0$. Fixed points of the system occur precisely

(footnote continued)
at intersections of the nullclines. In higher dimensions, nullclines are actually *nullsurfaces* and are much harder to visualize. In Figs. 10 and 11, we project onto a 2-dimenstional phase plane and are, therefore, looking at slices of the C_A and N^* nullsurfaces.
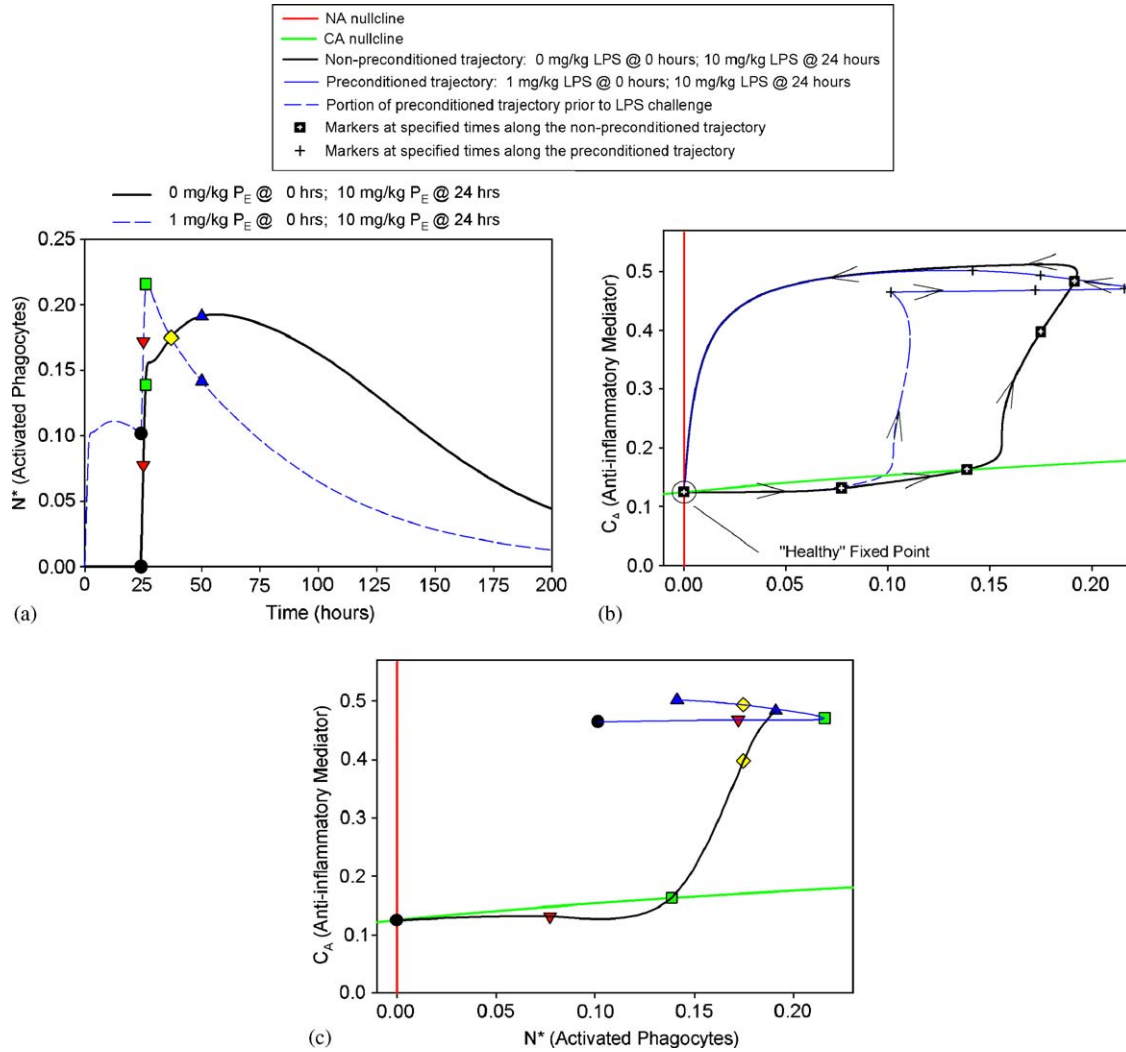
Fig. 10. Endotoxin tolerance (based on scenario 1) illustrated with the N^*-C_A phase plane. The specific markers represent the following: black circle = time point just prior to the administration of the challenge endotoxin dose, red upside down triangle = 1 h after the challenge dose, green square = 2 h after the challenge dose, yellow diamond = 13 h after challenge dose, and blue triangle = 26 h after challenge dose. In (a) the symbols described above are positioned on the N^* time courses of the non-preconditioned (solid) and preconditioned (dashed) simulations, where the preconditioned simulation time course falls below the non-preconditioned simulation time course just after the yellow diamond marker. In (b), the N^* nullcline (red; vertical line) and C_A nullcline (green; almost horizontal line) are shown along with two curves representing the trajectories of the non-preconditioned (black; thick) and preconditioned (blue; thin) simulations of scenario 1. The arrows signify which direction the trajectories are flowing in the phase plane. Although both trajectories end at the healthy fixed point after running their courses, the preconditioned (blue; thin) trajectory actually approaches the fixed point faster, resulting in tolerance. Several points are marked on the non-preconditioned and preconditioned trajectory with □ or +, respectively, denoting specific times prior to and after the time of the challenge endotoxin dose. These time points are shown again in (c) where they are color coded and connected to stress which ones belong on the non-preconditioned and preconditioned curves shown in (b). The black circle belonging to the curve of the non-preconditioned simulation shows that the trajectory is sitting at the healthy fixed point, where N^* and C_A are at their background levels. In comparison, the black circle belonging to the curve of the preconditioned simulation is sitting at a place in the phase plane where C_A is much greater than its baseline value. It is also a place where N^* is above its baseline, however, the trajectory is beginning to turn to the left toward the healthy fixed point and the challenge dose does not push the trajectory too far in the N^* direction. Comparing the other symbols in (c) on the two curves, the preconditioned trajectory is at a lower N^* level than the non-preconditioned curve at the same time just after the yellow diamond (compare the positions of the blue triangles with respect to N^*). This indicates that tolerance has occurred. Thus, the state the system is in at the time the challenge dose is given determines the outcome of the simulation.

viewpoint of a projection of the system to the N^*-C_A phase plane.

Likewise, Fig. 12a shows the N^*-D-C_A phase space to illustrate the rescue demonstrated in scenario 5 (Figs. 6a and b). The elevated amount of C_A in the system at the time of the challenge dose blunts the effect of the

potentially lethal dose, enabling the trajectory of the preconditioned simulation to remain in the basin of attraction of the healthy fixed point. In addition, Fig. 12b shows a similar rescue scenario in the N^*-D-C_A phase space along with the 2-dimensional separatrix consisting of the stable manifold of the saddle point of
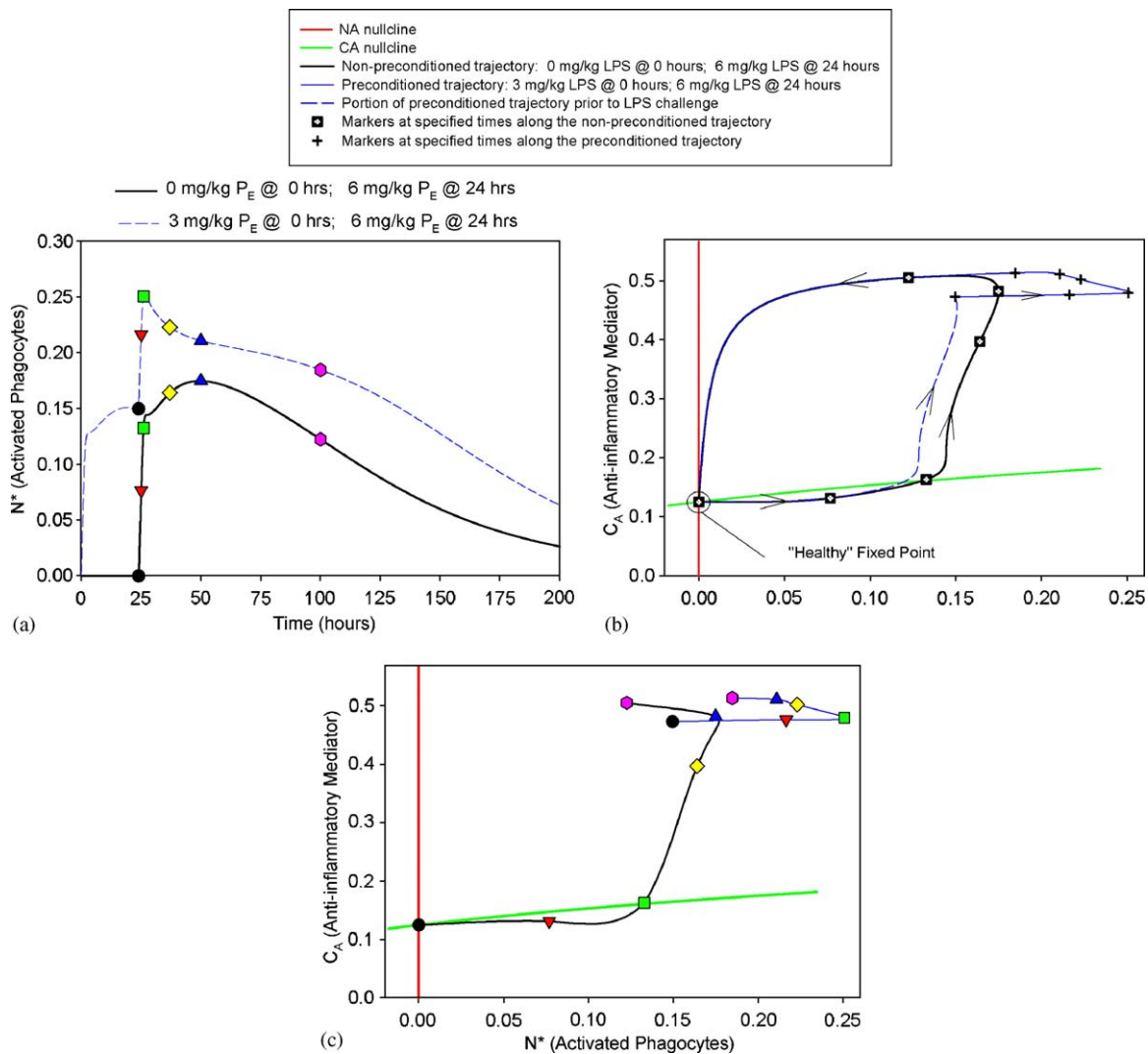
Fig. 11. Potentiation (based on scenario 6) illustrated with the N^*-C_A phase plane. The N^* time courses in (a) of the non-preconditioned (solid) and preconditioned (dashed) simulations illustrate that at each of the time markers, the N^* level of the preconditioned simulation is significantly above the non-preconditioned simulation levels. The explanation given in the caption for Fig. 10 is very similar to this panel, except that instead of the preconditioned trajectory outrunning the preconditioned simulation trajectory, it now trails the non-preconditioned trajectory for all time, as seen in (b). In addition, when comparing the symbols in panel (c), the levels of N^* (x-axis) are always greater in the preconditioned simulation. Although the position of the preconditioned simulation trajectory just prior to challenge is a place of elevated C_A, the level of N^* is quite high as well, and when the challenge is given, the new starting point of the preconditioned trajectory is pushed further to the right into high N^* territory. Consequently, the preconditioned trajectory cannot draw level with, much less pass, the non-preconditioned simulation.

the system.[3] The code for calculating the separatrix manifold was written in MATLAB, based on an algorithm presented by Krauskopf and Osinga (1999). The separatrix forms the border between the basins of attraction of the healthy and unhealthy states. This surface is exact (and thus invariant; see Strogatz (1994) for more details) only in the limit of $P_E = 0$. Nonetheless, since P_E decays quickly, this surface gives a reasonable estimate to the true separatrix location in (N^*-D-C_A) space for times that are not too close to endotoxin dose administration times.

Thus, the location of a trajectory a short time after a challenge dose, relative to the separatrix, determines the long-term fate of the system.

In all of the above discussions, it is clear that timing is very important to achieve tolerance. Therefore, we further investigate the dependence of tolerance on the amount of time between the preconditioning and challenge dose as well as the magnitude of preconditioning by examining a range of preconditioning doses and times at which they are given. In scenario 1, it was shown that a preconditioning dose of 1 mg/kg endotoxin 24 h prior to the challenge endotoxin dose of 10 mg/kg endotoxin produced endotoxin tolerance, marked by a decrease in the level of the model variable, N^*, compared with the non-preconditioned

---

[3]We chose not to use exactly the same trajectories produced in Fig. 12a because they followed the manifold too closely and it was difficult to visualize what exactly was happening.
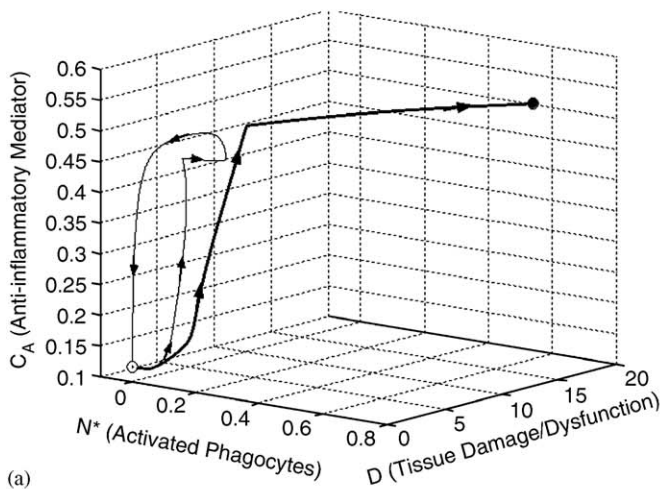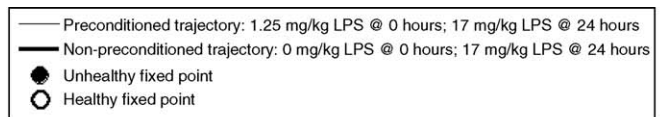
(a)
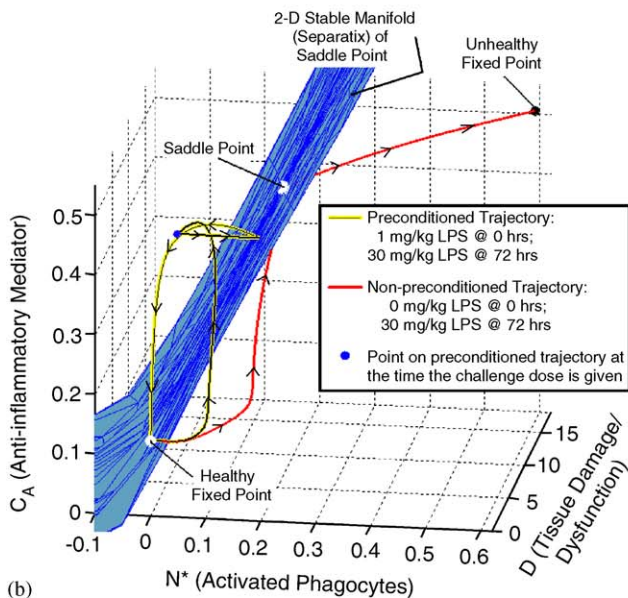
(b)

Fig. 12. Rescue scenario in the N^*-D-C_A phase space. (a) Using our simulations for scenario 5, this figure illustrates the concept of protection or rescue in the N^*-D-C_A phase space. The non-preconditioned trajectory (bold) is pushed into the basin of attraction for the unhealthy fixed point by the injection of the 17 mg/kg P_E dose at 24 h. The preconditioned trajectory, however, remains in the basin of attraction of the healthy fixed point. This is because the amount of C_A in the system just prior to the challenge dose is significantly above baseline and the effect of the 17 mg/kg hit of P_E is, therefore, blunted. (b) Using a slightly different but similar simulation to scenario 5, in which preconditioning again leads to rescue, we now show a portion of the 2-dimensional separatrix consisting of the stable manifold of the saddle point of the system (see text for more details). The preconditioned trajectory (black on yellow) stays on the healthy side of the surface after the challenge dose, while the challenge dose pushes the non-preconditioned trajectory (red) to the unhealthy side of the surface.
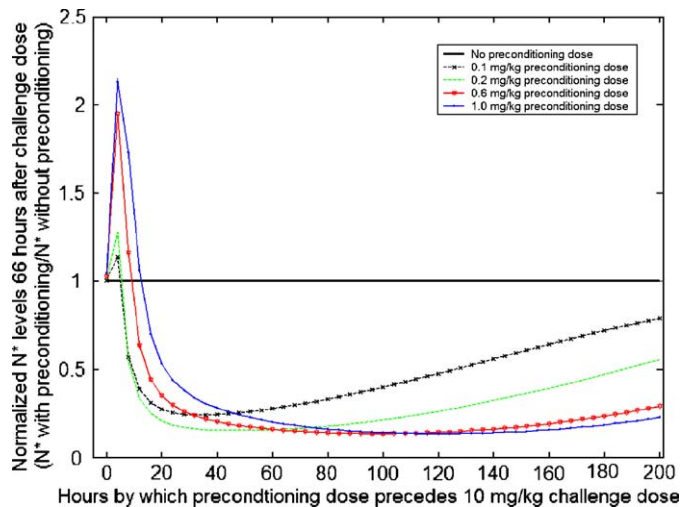

Fig. 13. Dependence of tolerance on preconditioning dose timing and magnitude. The solid, horizontal line marks the normalized level of N^* of the non-preconditioned simulation at 66 h after a 10 mg/kg challenge dose is given. Each individual curve shows the normalized level of N^* (recorded at 66 h after challenge) for a particular preconditioning dosage amount as a function of the time at which the dose was given prior to the challenge dose (from 0 to 200 h prior to challenge with 10 mg/kg endotoxin). Points on the curves that fall below the black line indicate that tolerance has occurred: The N^* value for a preconditioned simulation at 66 h after challenge is lower than that of the non-preconditioned simulation (represented by the solid, horizontal line). Those which are above the solid line produce potentiation instead. (See Section 5 for further details.)

simulation at a particular point in time, namely 66 h after challenge.

However, if we vary the amount of the preconditioning dose as well as the amount of time between the preconditioning dose and challenge dose, we see that there is a wide range of preconditioning doses and times at which they can be administered that also show a decrease in N^* at the time of comparison with the non-preconditioned simulation. Furthermore, the relationship between the size of the preconditioning dose and the time that it is given relative to the challenge dose is not obvious. In Fig. 13, we see that potentiation is evident for the range of preconditioning times that are close to the time the challenge dose is administered (approximately 0–15 h before challenge). Tolerance is observed when this interval is typically longer than 15 h. Interestingly, there is a brief interval (15–20 h before challenge) during which smaller preconditioning doses typically allow for more tolerance than larger doses do. For this case, the key point is that larger preconditioning doses elicit more inflammation than do smaller doses. Thus, for large doses, the inflammation is still high when the challenge dose is given, such that less tolerance is observed than for small doses. There is, however, a range of these preconditioning times (20–110 h before challenge) during which the relationship between the magnitude of the preconditioning dose and the amount of tolerance it elicits is not monotonic, due to a competition between the amount of inflammation and the amount of anti-inflam-

mation invoked by the preconditioning dose. Finally, for the range of preconditioning times from 110 to 200 h before challenge, the larger preconditioning doses exhibit more tolerance than the smaller doses. This is due to the fact that the smaller anti-inflammatory responses elicited by small preconditioning doses have worn off by these times, whereas for the larger preconditioning doses, the large degree of inflammation invoked has subsided by these times while the associated strong, prolonged anti-inflammation persists.

Thus, early second stimulation with endotoxin leads to potentiation of inflammation and consequently enhances lethality. Alternatively, if the second stimulus comes too late, significant tolerance fails to be induced. In our simulations, the build-up of C_A after a sub-lethal preconditioning endotoxin dose is transient, and C_A eventually settles back to equilibrium, along with the other effectors in the model. Thus, the preconditioned system response to late challenge stimuli is similar to that seen in non-preconditioned responses. In summary, we expect the existence of a window of possible challenge dose times and preconditioning magnitudes for which endotoxin tolerance is possible. Theoretical work is underway to mathematically analyse the nature of tolerance for more general dynamical systems.

6. Discussion

The preconditioning phenomena of potentiation and tolerance characterize acute inflammation in both rodents and humans (Copeland et al., 2005; Yadavalli et al., 2001); in humans, the latter phenomenon is often referred to as "immune paralysis" or "immune exhaustion", in which leukocytes–derived from patients with severe inflammation as measured by circulating pro-inflammatory cytokines—often produce low levels of these same inflammatory agents (Pinsky, 2001, 2004). In this paper, we show that an experimentally calibrated but highly reduced computational model for the acute inflammatory response (Reynolds et al., 2006; also see the Supplementary Materials) incorporates sufficient dynamic complexity to qualitatively reproduce a suite of experimental results associated with multiple endotoxin administrations in mice. Our success in matching experimental endotoxin tolerance results offers support for the biological relevance of the reduced model. Moreover, our simulations illustrate how the outcomes of endotoxin administration experiments can emerge as a natural consequence of the interactions of different components of the acute inflammatory response and also highlight the importance of including a dynamic late pro-inflammatory component in the model. We find that the relative time scales of the onset and decay of pro- and anti-inflammatory mediators are key determinants of outcomes in these experiments, as illustrated in the simulations and phase plane projections that we present. Finally, the results of our simulations involving potentiated responses (Fig. 7), low-dose protracted endotoxin infusion (Fig. 9), and

variations in the timing and amplitude of preconditioning doses (Fig. 13) yield predictions that remain to be verified experimentally.

Mathematical approaches to understanding endotoxin tolerance have not been extensively represented in the literature. However, in the work of Mayer and colleagues (Mayer et al., 1995) a simple two equation mathematical model of the immune response is presented and tolerance-like behavior is mentioned. Their model consists of immune cells (E) and target cells (T) which represent bacteria, for instance, and are inhibited by the immune cells. Although Mayer et al. do not consider endotoxin specifically and do not model anti-inflammatory effects, a form of tolerance is manifested in their model by a reduction in the growth of their target cells when a secondary infection is initiated, compared to the growth of the initial infection. This reduction is due to the fact that the concentration of the immune cells they model is elevated when the secondary infection is introduced. In fact, the secondary infection is initiated after the system has approached a steady state in which the immune cell concentration is high and the primary infection has been cleared. This simulation differs substantially from the situation we consider, in which a positive resolution corresponds to a return to the baseline rest state and endotoxin challenges come during transient excursions from this state induced by endotoxin preconditioning.

Much of the experimental literature regarding endotoxin tolerance focuses on the roles of *IL-10* and Transforming Growth Factor-$\beta 1$ (*TGF-$\beta 1$*), two potent anti-inflammatory cytokines (Grutz, 2005; Letterio et al., 2000; Randow et al., 1995; Zamora and Vodovotz, 2005) The possible roles that they each may have in endotoxin tolerance have been documented by Randow et al. (1995) and others (Cavaillon, 1995; Grutz, 2005; Sly et al., 2004). Our model suggests that the timing of doses for which tolerance will occur strongly depends on the time course of the anti-inflammatory mediators. For the experiments that we have reproduced, it is necessary for an anti-inflammatory influence to arise early on in the response, as is seen with *IL-10*, but also to remain elevated longer than *IL-10*. This latter feature might be true of mediators like *TGF-$\beta 1$* or possibly *IL-6*, which has been shown to have anti-inflammatory characteristics and is typically a cytokine produced relatively late in the course of an immune response (Xing et al., 1998).

It has been shown that preconditioning with *IL-10* protects mice from lethal endotoxin doses and also partially mimics endotoxin tolerance (Alves-Rosa et al., 2002; Cavaillon, 1995; Howard et al., 1993). However, this finding does not contradict our findings on the importance of a prolonged anti-inflammatory response for tolerance, since *IL-10* preconditioning leads to a different time course of anti-inflammatory mediators than occurs with the intrinsic immune response to endotoxin preconditioning. Indeed, if *IL-10* preconditioning introduces a significant presence of *IL-10* in the host during the time that a rather

toxic dose of endotoxin is administered, then it will suppress the pro-inflammatory response and thus enhance tolerance. Moreover, *IL-10* can either induce or activate *TGF-β1* (Letterio et al., 2000; Vodovotz and Barcellos-Hoff, 2001), thereby prolonging the overall anti-inflammatory effect.

As with other recently developed mathematical models of the acute inflammatory response (Chow et al., 2005; Clermont et al., 2004; Kumar et al., 2004) the model used here was calibrated to be consistent with relevant experimental literature. However, we do not claim that the model with the parameters we have chosen will be valid over a wide range of species, especially in regard to the differences in sensitivity to endotoxin. Mice can survive much higher doses of endotoxin than humans can, for instance. Not all the parameter ranges and estimates could be acquired from mouse data alone; however, whenever possible, we looked at literature and data regarding experimental work done in mice. In order to reproduce experiments carried out with other species such as humans, for example, it would be necessary to consult species specific data. See Supplementary Materials for more details regarding parameter choices.

Since our model is based on a simplified response system, it has certain limitations. For example, it is difficult to match specific biological mediators to the variables we have chosen, with the exception of endotoxin (P_E), and the model cannot predict quantitative measurements. However, we have tried to select parameters such that the time courses of our variable, N^*, are qualitatively similar to those suggested by experimental data to exist for early pro-inflammatory mediators like *TNF* and activated phagocytes. For example, our preliminary experimental data in rats suggest that the peak of activated neutrophils roughly matches that of circulating *TNF* (Lagoa et al., 2005). There are other apparent differences between our results and those in the literature. For instance, the reductions we show in N^* are not seen at the peak of its production, whereas the literature suggests that the reduction in *TNF* production is seen at its peak (90–120 min after challenge) (Sanchez-Cantu et al., 1989). However, since our early pro-inflammatory mediator is not solely based on *TNF*, exact comparison with experimental *TNF* data is simply not feasible. In addition, we demonstrate the induction of endotoxin tolerance by modeling the basic binding interaction of P_E with immune effector cells but without any special alterations that affect the clearance of P_E. Despite these limitations, our results highlight specific ways in which endotoxin tolerance and related phenomena can emerge from the timing and the overall interplay between mediators of the acute inflammatory response and illustrate the utility of a reduced model for the computational testing of hypotheses and generation of predictions related to this response.

Acknowledgments

Appendix A. Supplementary materials

Supplementary data associated with this article can be found in the online version at doi:10.1016/j.jtbi.2006.02.015.

References

Alexander, C., Rietschel, E.T., 2001. Bacterial lipopolysaccharides and innate immunity. J. Endotoxin Res. 7, 167–202.

Alves-Rosa, F., Vulcano, M., Beigier-Bompadre, M., Fernandez, G., Palermo, M., Isturiz, M.A., 2002. Interleukin-1beta induces in vivo tolerance to lipopolysaccharide in mice. Clin. Exp. Immunol. 128, 221–228.

Andersson, U., Wang, H., Palmblad, K., Aveberger, A.C., Bloom, O., Erlandsson-Harris, H., Janson, A., Kokkola, R., Zhang, M., Yang, H., Tracey, K.J., 2000. High mobility group 1 protein (HMG-1) stimulates proinflammatory cytokine synthesis in human monocytes. J. Exp. Med. 192, 565–570.

Bacon, G.E., Kenny, F.M., Murdaugh, H.V., Richards, C., 1973. Prolonged serum half-life of cortisol in renal failure. Johns Hopkins Med. J. 132, 127–131.

Balkhy, H.H., Heinzel, F.P., 1999. Endotoxin fails to induce IFN-gamma in endotoxin-tolerant mice: deficiencies in both IL-12 heterodimer production and IL-12 responsiveness. J. Immunol. 162, 3633–3638.

Beeson, P.B., 1947. Tolerance to bacterial pyrogens: I. Factors influencing its development. J. Exp. Med. 86, 29–38.

Berg, D.J., Kuhn, R., Rajewsky, K., Muller, W., Menon, S., Davidson, N., Grunig, G., Rennick, D., 1995. Interleukin-10 is a central regulator of the response to LPS in murine models of endotoxic shock and the Shwartzman reaction but not endotoxin tolerance. J. Clin. Invest. 96, 2339–2347.

Bocci, V., 1991. Interleukins. Clinical pharmacokinetics and practical implications. Clin. Pharmacokinet. 21, 274–284.

Bumiller, A., Gotz, F., Rohde, W., Dorner, G., 1999. Effects of repeated injections of interleukin 1beta or lipopolysaccharide on the HPA axis in the newborn rat. Cytokine 11, 225–230.

Cavaillon, J.-M., 1995. The nonspecific nature of endotoxin tolerance. Trends Microbiol. 3, 320–324.

Cavaillon, J.M., Pitton, C., Fitting, C., 1994. Endotoxin tolerance is not a LPS-specific phenomenon: partial mimicry with IL-1, IL-10 and TGF-beta. J. Endotoxin Res. 1, 21–29.

Chow, C.C., Clermont, G., Kumar, R., Lagoa, C., Tawadrous, Z., Gallo, D., Betten, B., Bartels, J., Constantine, G., Fink, M.P., Billiar, T.R., Vodovotz, Y., 2005. The acute inflammatory response in diverse shock States. Shock 24, 74–84.

Clermont, G., Bartels, J., Kumar, R., Constantine, G., Vodovotz, Y., Chow, C., 2004. In silico design of clinical trials: a method coming of age. Crit. Care Med. 32, 2061–2070.

Copeland, S., Warren, H.S., Lowry, S.F., Calvano, S.E., Remick, D., 2005. Acute inflammatory response to endotoxin in mice and humans. Clin. Diagn. Lab Immunol. 12, 60–67.

Coxon, A., Tang, T., Mayadas, T.N., 1999. Cytokine-activated endothelial cells delay neutrophil apoptosis in vitro and in vivo. A role for granulocyte/macrophage colony-stimulating factor. J. Exp. Med. 190, 923–934.

Cross, A.S., 2002. Endotoxin tolerance-current concepts in historical perspective. J. Endotoxin Res. 8, 83–98.

Degryse, B., Bonaldi, T., Scaffidi, P., Muller, S., Resnati, M., Sanvito, F., Arrigoni, G., Bianchi, M.E., 2001. The high mobility group (HMG) boxes of the nuclear protein HMG1 induce chemotaxis and cytoskeleton reorganization in rat smooth muscle cells. J. Cell Biol. 152, 1197–1206.

Eng, R.H., Smith, S.M., Fan-Havard, P., Ogbara, T., 1993. Effect of antibiotics on endotoxin release from gram-negative bacteria. Diagn. Microbiol. Infect. Dis. 16, 185–189.

Ermentrout, G.B., 2002. Simulating, Analyzing, and Animating Dynamical Systems: A Guide to XPPAUT for Researchers and Students, first ed. Soc for Industrial & Applied Math, Philadelphia.

Fuchs, A.C., Granowitz, E.V., Shapiro, L., Vannier, E., Lonnemann, G., Angel, J.B., Kennedy, J.S., Rabson, A.R., Radwanski, E., Affrime, M.B., Cutler, D.L., Grint, P.C., Dinarello, C.A., 1996. Clinical, hematologic, and immunologic effects of interleukin-10 in humans. J. Clin. Immunol. 16, 291–303.

Grutz, G., 2005. New insights into the molecular mechanism of interleukin-10-mediated immunosuppression. J. Leukoc. Biol. 77, 3–15.

Howard, M., Muchamuel, T., Andrade, S., Menon, S., 1993. Interleukin 10 protects mice from lethal endotoxemia. J. Exp. Med. 177, 1205–1208.

Huhn, R.D., Radwanski, E., Gallo, J., Affrime, M.B., Sabo, R., Gonyo, G., Monge, A., Cutler, D.L., 1997. Pharmacodynamics of subcutaneous recombinant human interleukin-10 in healthy volunteers. Clin. Pharmacol. Ther. 62, 171–180.

Isler, P., de Rochemonteix, B.G., Songeon, F., Boehringer, N., Nicod, L.P., 1999. Interleukin-12 production by human alveolar macrophages is controlled by the autocrine production of interleukin-10. Am. J. Respir. Cell Mol. Biol. 20, 270–278.

Iversen, M.H., Hahn, R.G., 1999. Acute effects of vitamin A on the kinetics of endotoxin in conscious rabbits. Intensive Care Med. 25, 1160–1164.

Janeway Jr., C.A., Medzhitov, R., 2002. Innate immune recognition. Annu. Rev. Immunol. 20, 197–216.

Janeway Jr., C.A., Travers, P., Walport, M., Shlomchik, M., 2001. Immunobiology: The Immune System in Health and Disease, fifth ed. Garland Publishing, New York.

Kariko, K., Weissman, D., Welsh, F.A., 2004. Inhibition of toll-like receptor and cytokine signaling—a unifying theme in ischemic tolerance. J. Cereb. Blood Flow Metab. 24, 1288–1304.

Keel, M., Schregenberger, N., Steckholzer, U., Ungethum, U., Kenney, J., Trentz, O., Ertel, W., 1996. Endotoxin tolerance after severe injury and its regulatory mechanisms. J. Trauma 41, 430–437.

Krauskopf, B., Osinga, H., 1999. Two-dimensional global manifolds of vector fields. Chaos. 9, 768–774.

Kumar, R., Clermont, G., Vodovotz, Y., Chow, C.C., 2004. The dynamics of acute inflammation. J. Theor. Biol. 230, 145–155.

Lagoa, C.E., Chow, C.C., Bartels, J., Barrat, A., Kumar, R., Day, J., Rubin, J., Constantine, G., Chang, S., Fink, M.P., Billiar, T.R., Clermont, G., Vodovotz, Y., 2005. Mathematical models predict the course of the inflammatory response in rats subjected to trauma-hemorrhagic shock, and to anti-tumor necrosis factor alpha therapy in endotoxemia (abstract). J. Crit. Care 20, 393–394.

Leon, P., Redmond, H.P., Shou, J., Daly, J.M., 1992. Interleukin 1 and its relationship to endotoxin tolerance. Arch. Surg. 127, 146–151.

Letterio, J.J., Vodovotz, Y., Bogdan, C., 2000. TGF-beta and IL-10: inhibitory cytokines regulating immunity and the response to infection. In: Henderson, H. (Ed.), Novel Cytokine Inhibitors Birkhauser. Verlag, Basel, pp. 217–242.

Matzinger, P., 2002. The danger model: a renewed sense of self. Science 296, 301–305.

Mayer, H., Zaenker, K.S., an der Heiden, U., 1995. A basic mathematical model of the immune response. Chaos 5, 155–161.

Mendez, C., Kramer, A.A., Salhab, K.F., Valdes, G.A., Norman, J.G., Tracey, K.J., Carey, L.C., 1999. Tolerance to shock: an exploration of mechanism. Ann. Surg. 229, 843–849.

Morrison, D.C., Ryan, J.L., 1987. Endotoxins and disease mechanisms. Annu. Rev. Med. 38, 417–432.

Nathan, C., 2002. Points of control in inflammation. Nature 420, 846–852.

Nathan, C., Sporn, M., 1991. Cytokines in context. J. Cell Biol. 113, 981–986.

National Research Council, 1992. Animal models for use in detecting immunotoxic potential and determining mechanisms of action biologic markers. In: Immunotoxicology. National Academy Press, Washington, p. 95.

Parker, S.J., Watkins, P.E., 2001. Experimental models of gram-negative sepsis. Br. J. Surg. 88, 22–30.

Parrillo, J.E., 1993. Pathogenetic mechanisms of septic shock. N. Engl. J. Med. 328, 1471–1477.

Pinsky, M.R., 2001. Sepsis: a pro- and anti-inflammatory disequilibrium syndrome. Contrib. Nephrol., 354–366.

Pinsky, M.R., 2004. Dysregulation of the immune response in severe sepsis. Am. J. Med. Sci. 328, 220–229.

Randow, F., Syrbe, U., Meisel, C., Krausch, D., Zuckermann, H., Platzer, C., Volk, H.D., 1995. Mechanism of endotoxin desensitization: involvement of interleukin 10 and transforming growth factor beta. J. Exp. Med. 181, 1887–1892.

Rayhane, N., Fitting, C., Cavaillon, J.-M., 1999. Dissociation of IFN-gamma from IL-12 and IL-18 production during endotoxin tolerance. J. Endotoxin Res. 5, 319–324.

Reynolds, A., Rubin, J., Clermont, G., Day, J., Ermentrout, B., 2006. A reduced mathematical model of the acute inflammatory response: I. Derivation of the model and analysis of anti-inflammation. J. Theor. Biol. in press, doi:10.1016/j.jtbi.2006.02.016.

Sanchez-Cantu, L., Rode, H.N., Christou, N.V., 1989. Endotoxin tolerance is associated with reduced secretion of tumor necrosis factor. Arch. Surg. 124, 1432–1435.

Schade, F.U., Flach, R., Flohe, S., Majetschak, M., Kreuzfelder, E., Dominguez-Fernandez, E., Borgermann, J., Obertacke, U., 1999. Endotoxin tolerance. In: Brade, M., Opal, V. (Eds.), Endotoxin in Health and Disease. Marcel Dekker, New York, pp. 751–767.

Senaldi, G., Shaklee, C.L., Guo, J., Martin, L., Boone, T., Mak, T.W., Ulich, T.R., 1999. Protection against the mortality associated with disease models mediated by TNF and IFN-gamma in mice lacking IFN regulatory factor-1. J. Immunol. 163, 6820–6826.

Sly, L.M., Rauh, M.J., Kalesnikoff, J., Song, C.H., Krystal, G., 2004. LPS-induced upregulation of SHIP is essential for endotoxin tolerance. Immunity 21, 227–239.

Strogatz, S.H., 1994. Nonlinear Dynamics and Chaos: with Applications to Physics, Biology, Chemistry, and Engineering. Westview Press, Cambridge.

Vodovotz, Y., Barcellos-Hoff, M.H., 2001. Direct and indirect modulation of the inducible nitric oxide synthase by nitric oxide: feedback mechanisms in inflammation. In: Salvemini, Billiar, V. (Eds.), Nitric Oxide and Inflammation. Birkhauser-Verlag, Basel, pp. 41–58.

Vogel, S.N., Kaufman, E.N., Tate, M.D., Neta, R., 1988. Recombinant interleukin-1 alpha and recombinant tumor necrosis factor alpha synergize in vivo to induce early endotoxin tolerance and associated hematopoietic changes. Infect. Immun. 56, 2650–2657.

Wang, H., Bloom, O., Zhang, M., Vishnubhakat, J.M., Ombrellino, M., Che, J., Frazier, A., Yang, H., Ivanova, S., Borovikova, L., Manogue, K.R., Faist, E., Abraham, E., Andersson, J., Andersson, U., Molina, P.E., Abumrad, N.N., Sama, A., Tracey, K.J., 1999. HMG-1 as a late mediator of endotoxin lethality in mice. Science 285, 248–251.

Warner, A.E., DeCamp Jr., M.M., Molina, R.M., Brain, J.D., 1988. Pulmonary removal of circulating endotoxin results in acute lung injury in sheep. Lab. Invest. 59, 219–230.

Weisstein, E.W., 2006. Basin of attraction. In: MathWorld–A Wolfram Web Resource. Date Accessed: 1-30-2006. http://mathworld.wolfram.com/BasinofAttraction.html.

West, M.A., Heagy, W., 2002. Endotoxin tolerance: a review. Crit. Care Med. 30, S64–S73.

Wysocka, M., Robertson, S., Riemann, H., Caamano, J., Hunter, C., Mackiewicz, A., Montaner, L.J., Trinchieri, G., Karp, C.L., 2001. IL-12 suppression during experimental endotoxin tolerance: dendritic cell loss and macrophage hyporesponsiveness. J. Immunol. 166, 7504–7513.

Xing, Z., Gauldie, J., Cox, G., Baumann, H., Jordana, M., Lei, X.F., Achong, M.K., 1998. IL-6 is an antiinflammatory cytokine required

for controlling local or systemic acute inflammatory responses. J. Clin. Invest. 101, 311–320.

Yadavalli, G.K., Auletta, J.J., Gould, M.P., Salata, R.A., Lee, J.H., Heinzel, F.P., 2001. Deactivation of the innate cellular immune response following endotoxic and surgical injury. Exp. Mol. Pathol. 71, 209–221.

Yoshida, M., Roth, R.I., Levin, J., 1995. The effect of cell-free hemoglobin on intravascular clearance and cellular, plasma, and organ distribution of bacterial endotoxin in rabbits. J. Lab. Clin. Med. 126, 151–160.

Zamora, R., Vodovotz, Y., 2005. Transforming growth factor-beta in critical illness. Crit. Care Med. 33 (suppl), S478–S481.

Zervos, E.E., Kramer, A.A., Salhab, K.F., Norman, J.G., Carey, L.C., Rosemurgy, A.S., 1999. Sublethal hemorrhage blunts the inflammatory cytokine response to endotoxin in a rat model. J. Trauma 46, 145–149.